

Contact Mechanics and Elements of Tribology

Lecture 3. *Contact and Mechanics of Materials*

Vladislav A. Yastrebov

*Mines Paris - PSL, CNRS
Centre des Matériaux, Evry, France*

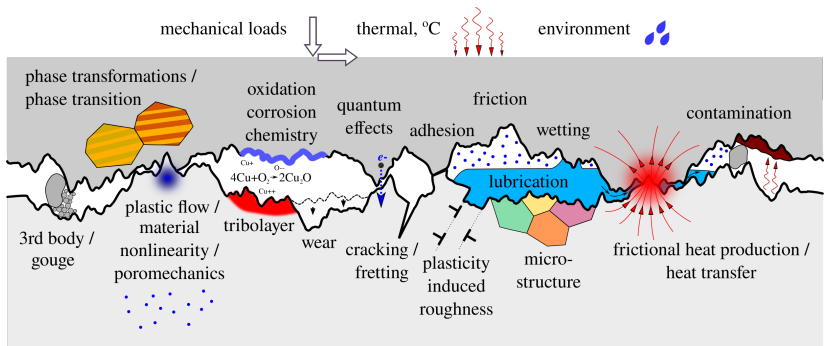


@ Centre des Matériaux (& virtually)
February 25, 2025



Creative Commons BY
Vladislav A. Yastrebov

Interface physics



Tribological properties stem from this complex multi-scale physics of interfaces and near-surface layers^[1]

[1] Vakis, Yastrebov, Scheibert, Nicola, Dini, Minfray, Almqvist, Paggi, Lee, Limbert, Molinari, Anciaux, Aghababaei, Echeverri Restrepo, Papangelo, Cammarata, Nicolini, Putignano, Carbone, Stupkiewicz, Lengiewicz, Costagliola, Bosia, Guarino, Pugno, Muser, Ciavarella, 2018. **Modeling and simulation in tribology across scales: An overview.** Tribology International, 125:169-199 (2018).

Outline

- Elastic-plastic contact
- Viscoelastic contact
- Frictional strengthening or time-dependent contact

Plasticity

Onset of plastic yielding

Hertz contact: body of revolution

- Onset of plasticity for pressure

$$p_Y = 1.6\sigma_Y$$

- Associated force

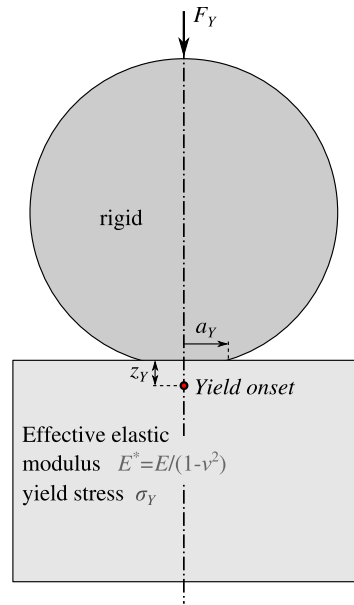
$$F_Y = \frac{1.6^3 \pi^3 R^2}{6} \left(\frac{\sigma_Y}{E^*} \right)^2 \sigma_Y$$

- Associated contact radius

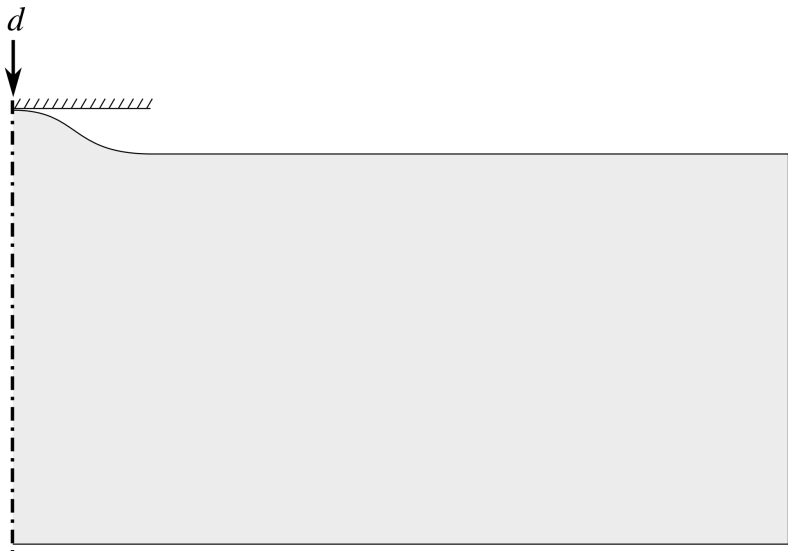
$$a_Y = \frac{1.6\pi R}{2} \frac{\sigma_Y}{E^*}$$

- Plastic flow starts at the depth

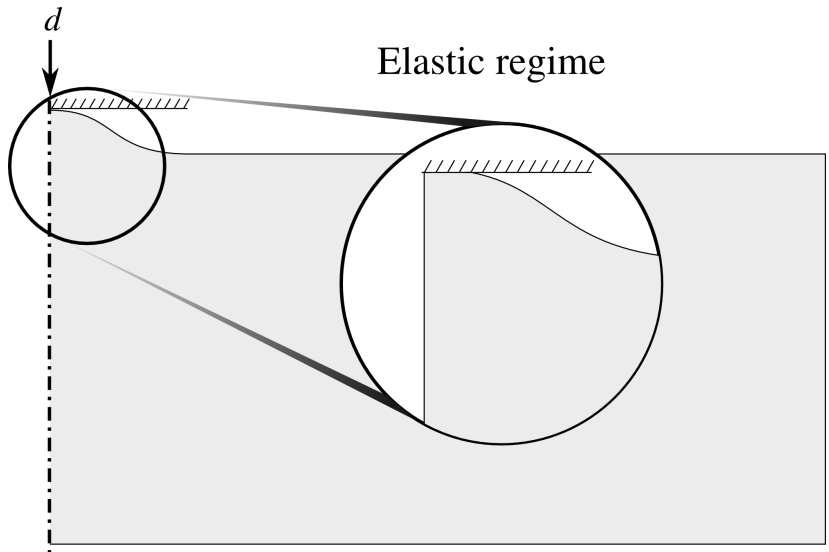
$$z_Y \approx 1.21R \frac{\sigma_Y}{E^*}$$



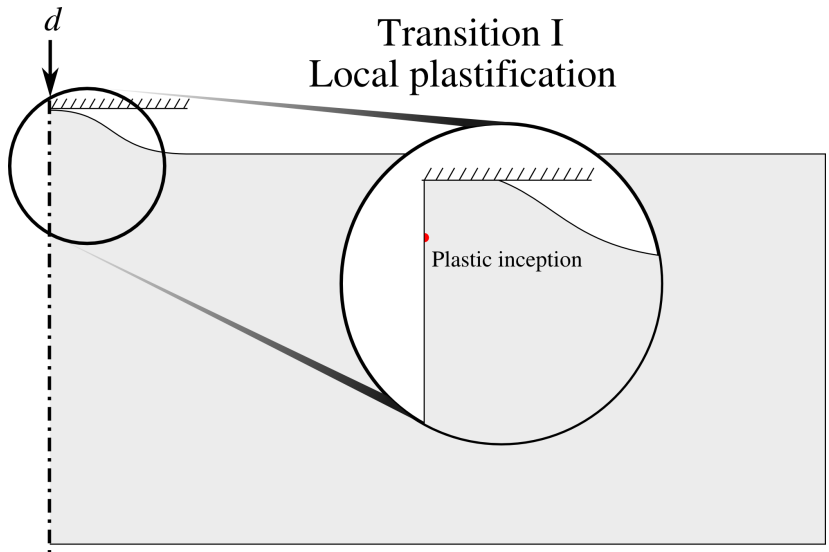
Elasto-plastic transition in contact



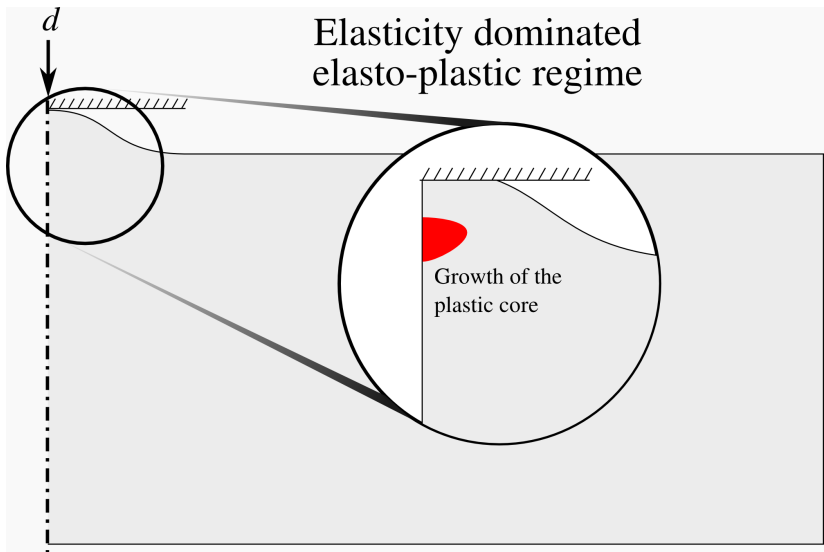
Elasto-plastic transition in contact



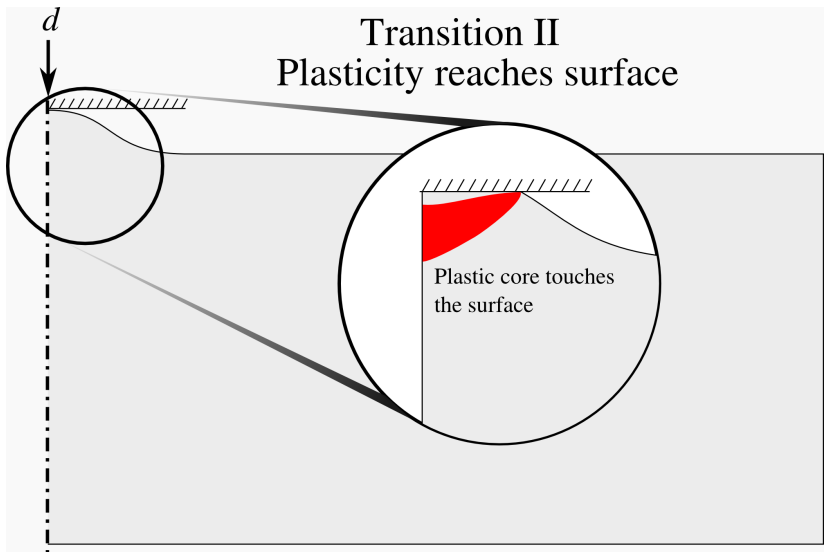
Elasto-plastic transition in contact



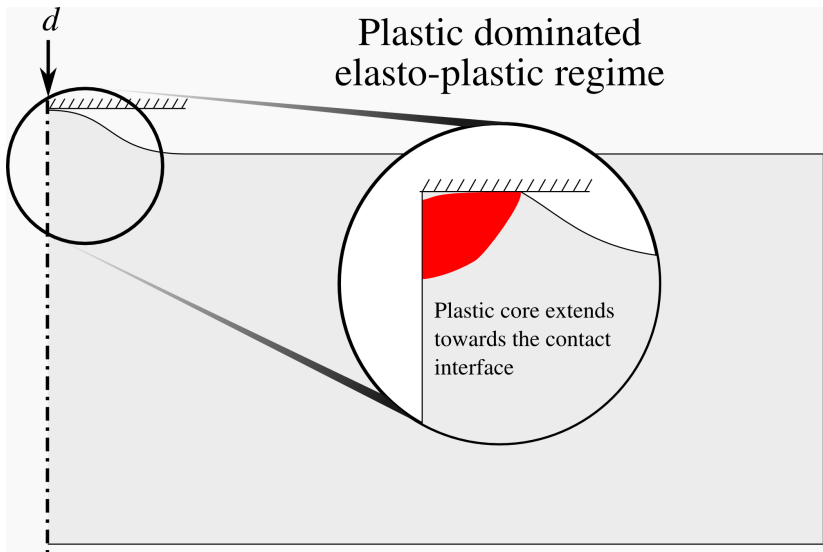
Elasto-plastic transition in contact



Elasto-plastic transition in contact

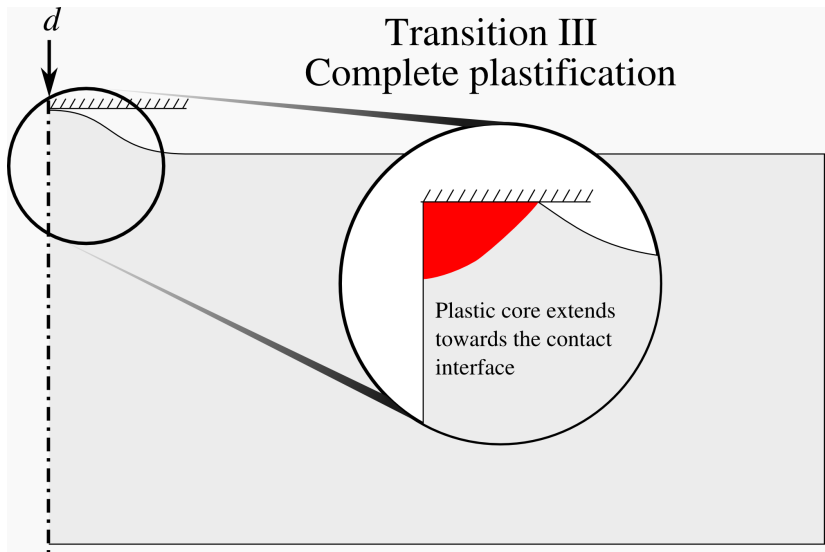


Elasto-plastic transition in contact

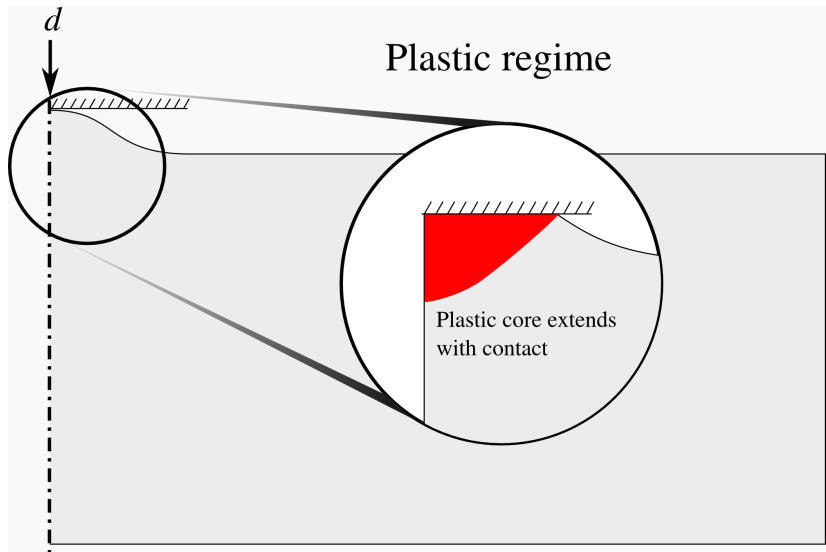


Elasto-plastic transition in contact

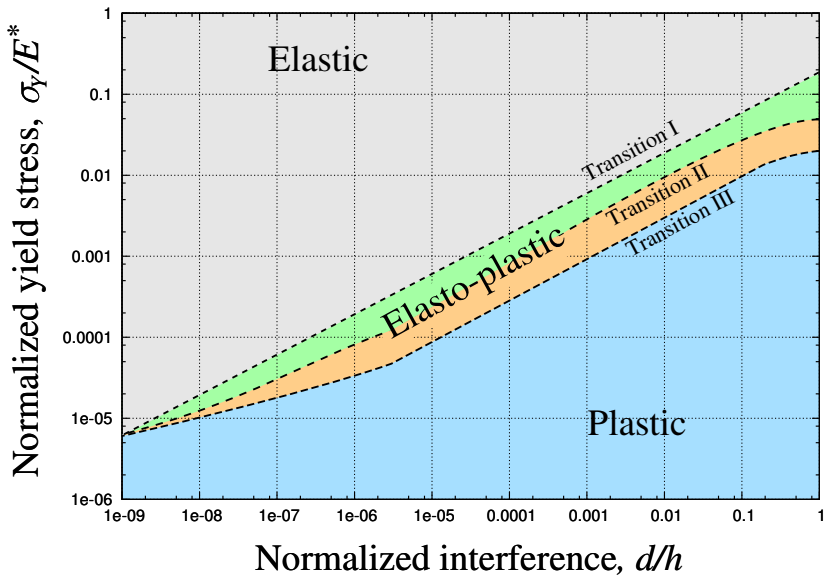
Transition III Complete plastification



Elasto-plastic transition in contact

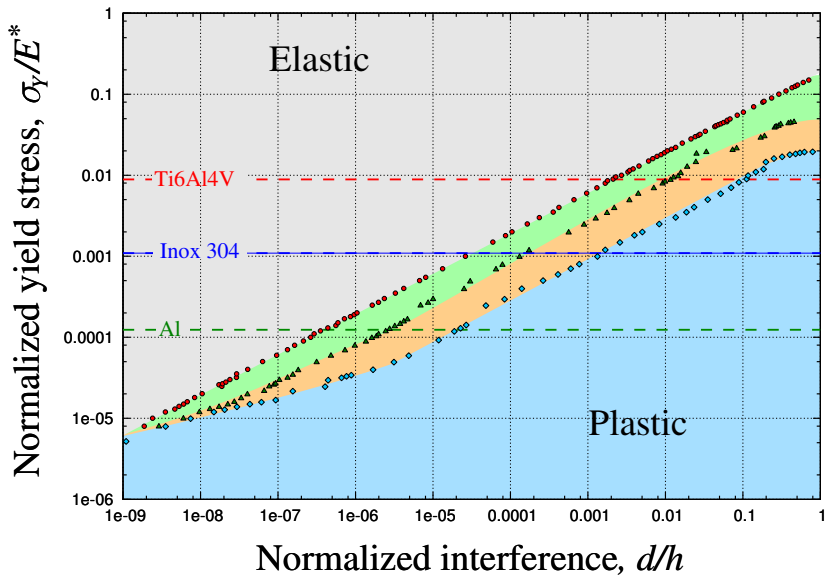


Elasto-plastic transition in contact



Deformation map for a sinusoidal asperity constructed with M. Liu, H. Proudhon
 $h/\lambda = 0.1$

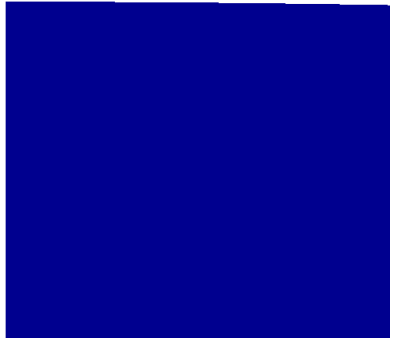
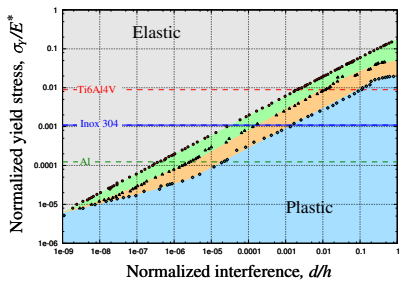
Elasto-plastic transition in contact



Deformation map for a sinusoidal asperity constructed with M. Liu, H. Proudhon

Elasto-plastic transition in contact

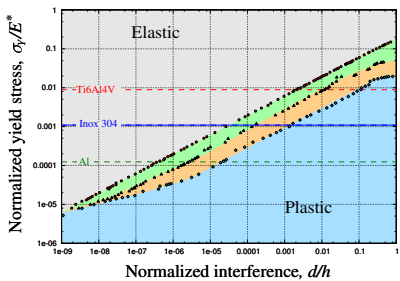
Case: $\sigma_Y/E = 0.0005$



Evolution of the plastic zone in a sinusoidal asperity in contact with a rigid flat

Elasto-plastic transition in contact

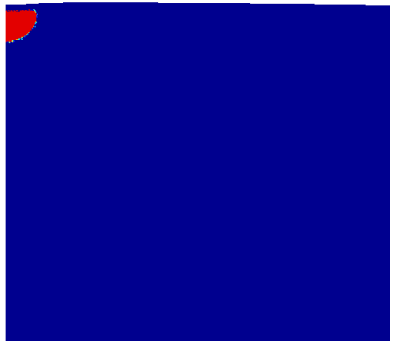
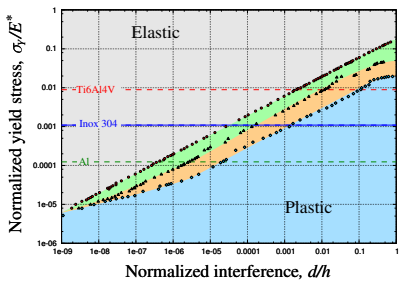
Case: $\sigma_Y/E = 0.0005$



Evolution of the plastic zone in a sinusoidal asperity in contact with a rigid flat

Elasto-plastic transition in contact

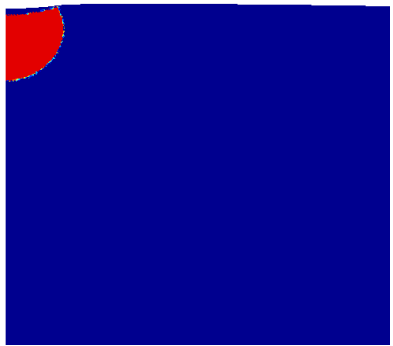
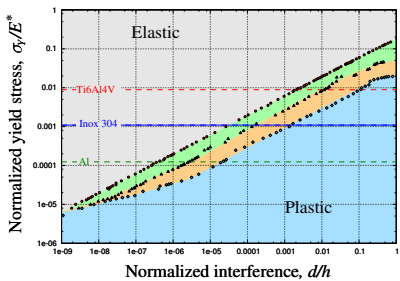
Case: $\sigma_Y/E = 0.0005$



Evolution of the plastic zone in a sinusoidal asperity in contact with a rigid flat

Elasto-plastic transition in contact

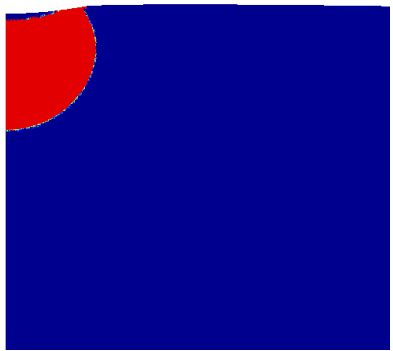
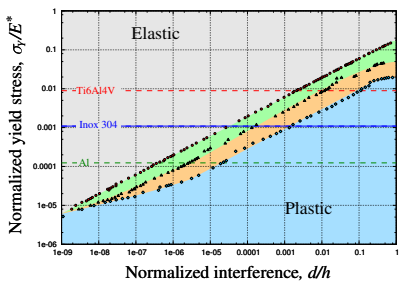
Case: $\sigma_Y/E = 0.0005$



Evolution of the plastic zone in a sinusoidal asperity in contact with a rigid flat

Elasto-plastic transition in contact

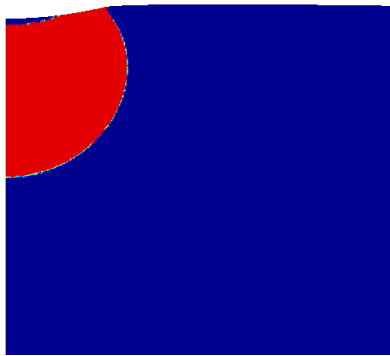
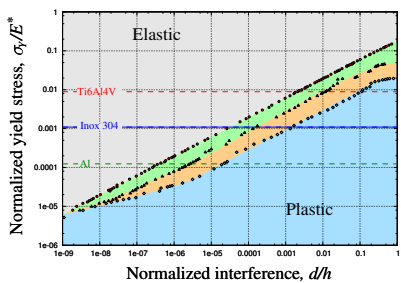
Case: $\sigma_Y/E = 0.0005$



Evolution of the plastic zone in a sinusoidal asperity in contact with a rigid flat

Elasto-plastic transition in contact

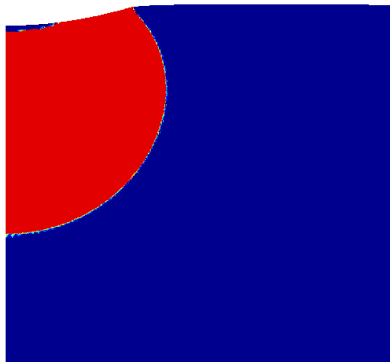
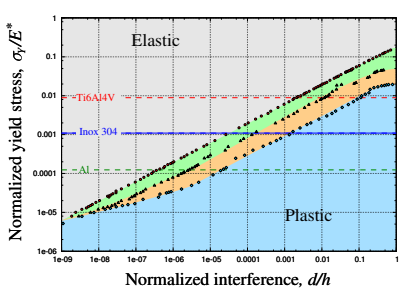
Case: $\sigma_Y/E = 0.0005$



Evolution of the plastic zone in a sinusoidal asperity in contact with a rigid flat

Elasto-plastic transition in contact

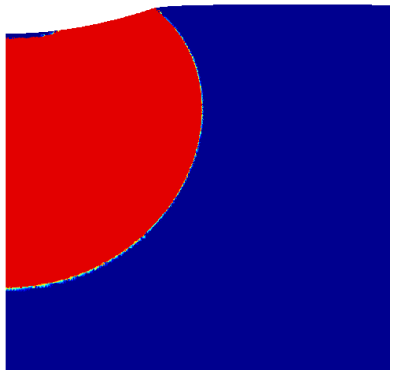
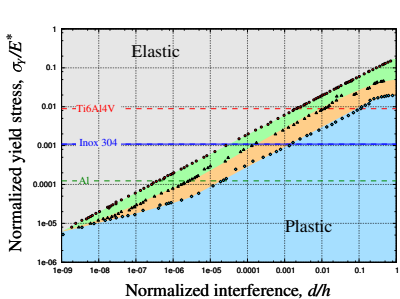
Case: $\sigma_Y/E = 0.0005$



Evolution of the plastic zone in a sinusoidal asperity in contact with a rigid flat

Elasto-plastic transition in contact

Case: $\sigma_Y/E = 0.0005$



Evolution of the plastic zone in a sinusoidal asperity in contact with a rigid flat

Elastic-plastic normal contact: hardness

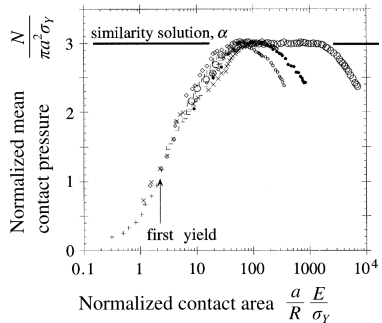
- Hardness \sim saturated plastic contact
- Recall: Vickers hardness
 $HV = N/A$
- Similarity solution^[1]

$$\frac{N}{\pi a^2 \sigma_Y} = F \left(\frac{a}{R} \frac{E}{\sigma_y} \right)$$

- Hardness $H \approx 3\sigma_Y$

[1] Hill R., Storøakers B., Zdunek A.B. A theoretical study of the Brinell hardness test. Proc R Soc Lond A 436 (1989)

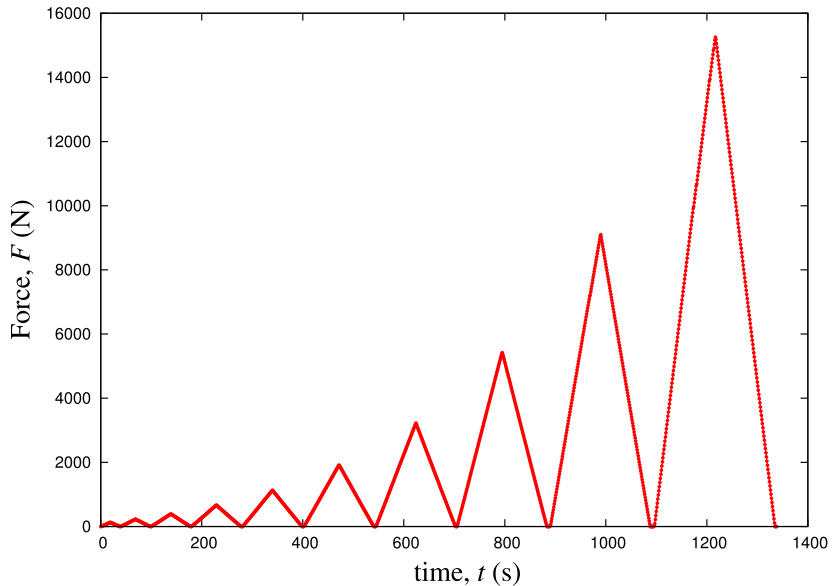
[2] Tabor, D. The Hardness of Metals. Oxford at the Clarendon Press (2000).



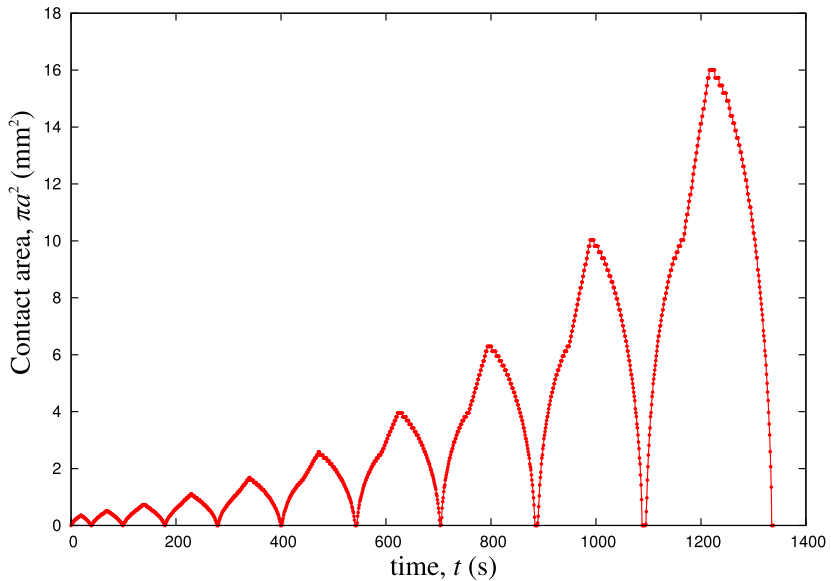
Simulation of spherical indentation of elasto-plastic solid with power-law hardening^[2]

[3] Mesarovic S., N. Fleck, Spherical Indentation of Elastic-Plastic Solids, Proc R Soc Lond A 455 (1999)

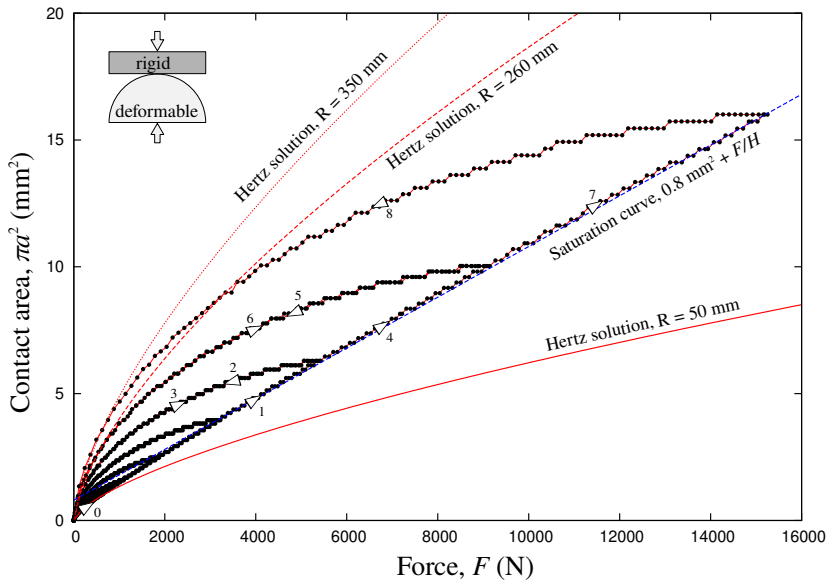
Elasto-plastic contact under cyclic load



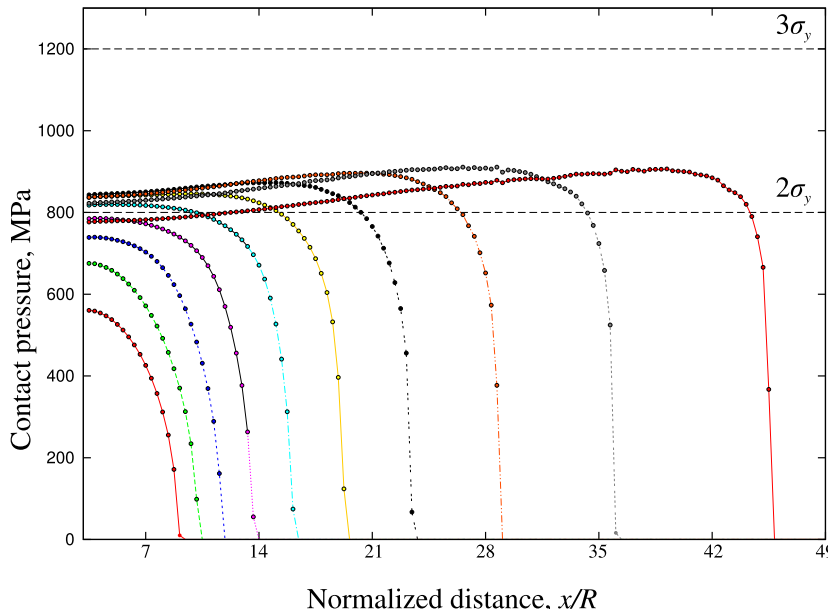
Elasto-plastic contact under cyclic load



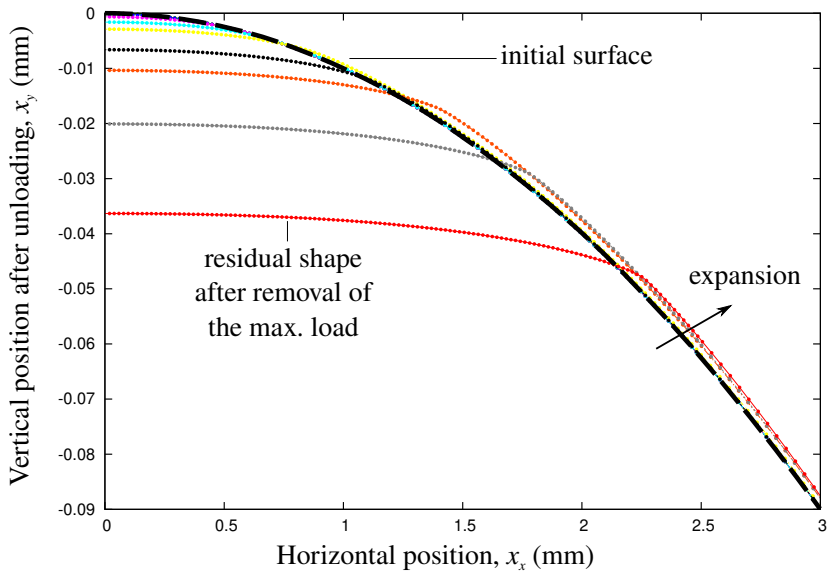
Elasto-plastic contact under cyclic load



Elasto-plastic contact under cyclic load



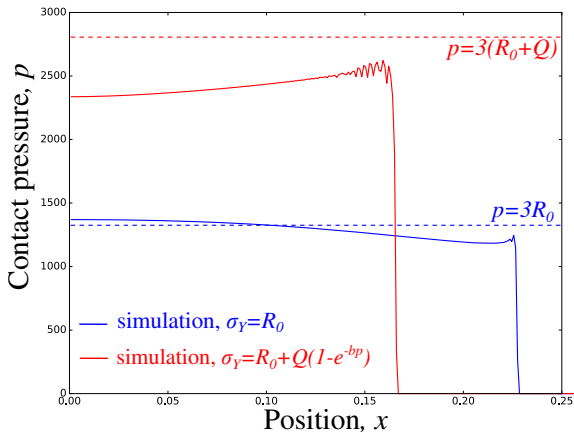
Elasto-plastic contact under cyclic load



Finer-mesh and hardening effect

Two hardening models

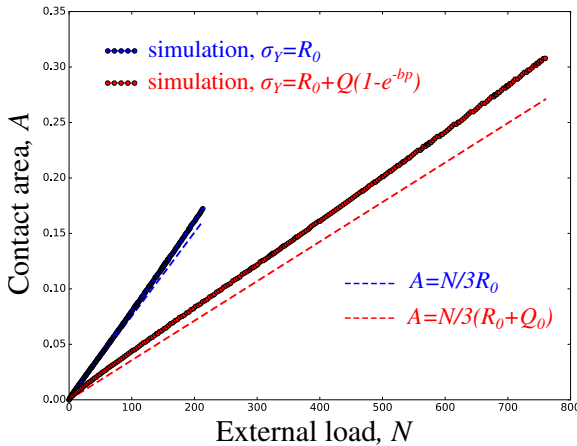
- perfect plasticity $R = R_0$
- non-linear hardening with saturation $R(p) = R_0 + Q(1 - \exp(-bp))$



Finer-mesh and hardening effect

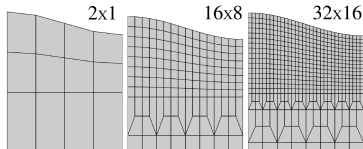
Two hardening models

- perfect plasticity $R = R_0$
- non-linear hardening with saturation $R(p) = R_0 + Q(1 - \exp(-bp))$

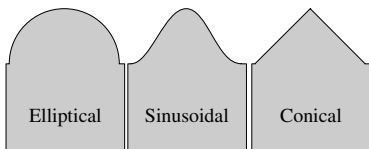


Deformation in fully plastic regime

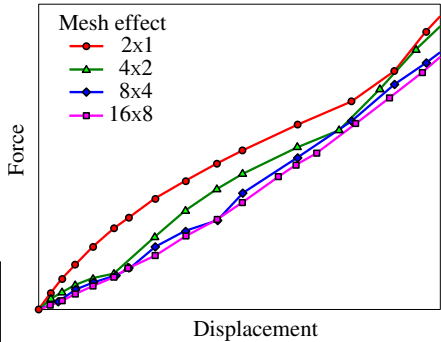
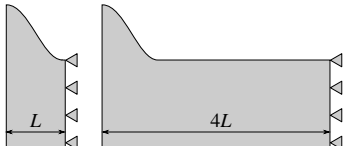
✓ Mesh effect



Shape effect



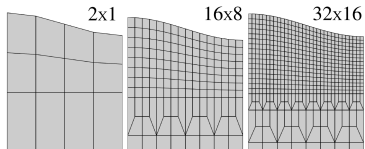
Edge effect



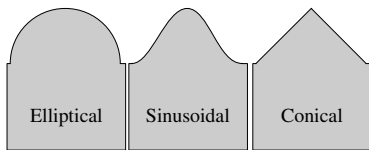
[1] V. A. Yastrebov, J. Durand, H. Proudhon, G. Cailletaud, CR Mecan, 339:473-490 (2011)

Deformation in fully plastic regime

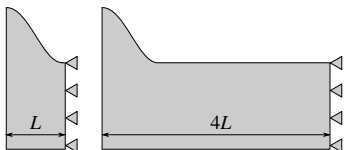
Mesh effect



✓ Shape effect



Edge effect



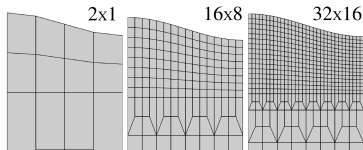
Relative contact area
0% 80%

Shape effect
— Elliptic
— Sinusoidal
— Conical

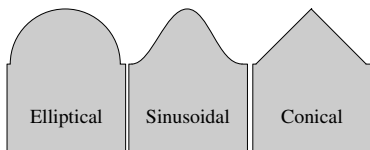
[1] V. A. Yastrebov, J. Durand, H. Proudhon, G. Cailletaud, CR Mecan, 339:473-490 (2011)

Deformation in fully plastic regime

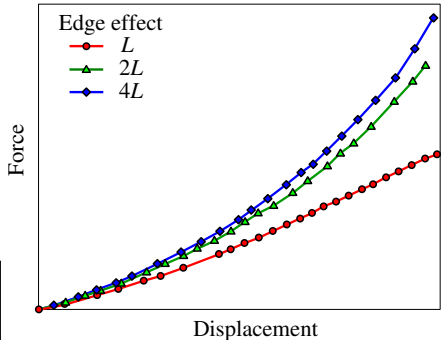
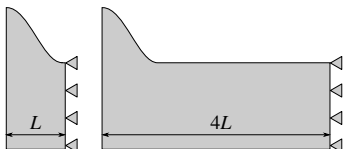
Mesh effect



Shape effect



✓ Edge effect



[1] V. A. Yastrebov, J. Durand, H. Proudhon, G. Cailletaud, CR Mecan, 339:473-490 (2011)

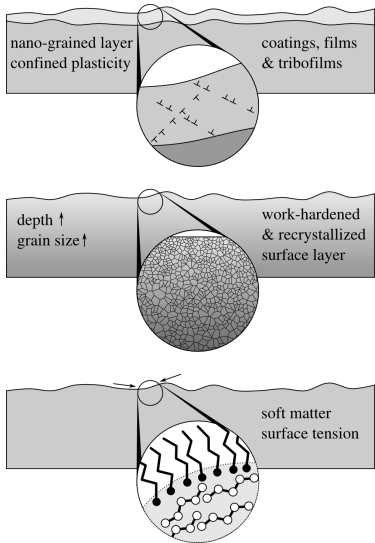
Near-surface vs bulk deformation

Material aspects

- Cold worked surface + recrystallized:
smaller grains near the surface,
Hall-Petch effect
- Thin coating films:
nanograined, confined plasticity,
Hall-Petch effect
- Oxides:
brittle hard films

Geometrical aspects

- Roughness of all nature
- Indentation by asperities:
confined plastic zone, high plastic strain gradients



Onset of yielding at atomic scale

Hertz contact: body of revolution

- Onset of plasticity for pressure

$$p_Y = 1.6\sigma_Y$$

- Associated force

$$F_Y = \frac{1.6^3 \pi^3 R^2}{6} \left(\frac{\sigma_Y}{E^*} \right)^2 \sigma_Y$$

- Associated contact radius

$$a_Y = \frac{1.6\pi R}{2} \frac{\sigma_Y}{E^*}$$

- Plastic flow starts at the depth

$$z_Y \approx 1.21R \frac{\sigma_Y}{E^*}$$

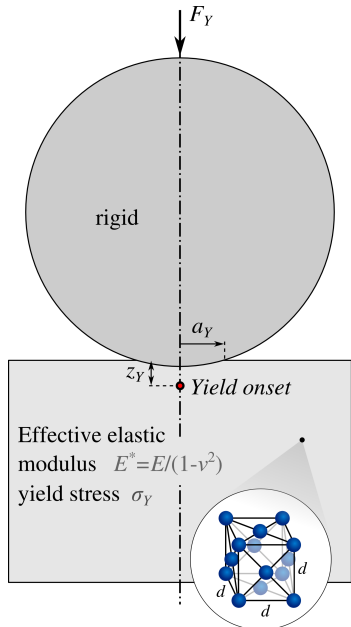
- Example: golden asperity

$$E^* \approx 96 \text{ GPa}, \quad \sigma_Y \approx 140 \text{ MPa}, \quad d \approx 4.1 \text{ \AA}$$

$$R = 10 \mu\text{m}$$

$$F_Y \approx 3.8 \mu\text{N}, \quad z_Y \approx 18 \text{ nm}, \quad a_Y \approx 36 \text{ nm}$$

$$z_Y \approx 45d, \quad a_Y \approx 115d$$



Onset of yielding at atomic scale

Hertz contact: body of revolution

- Onset of plasticity for pressure

$$p_Y = 1.6\sigma_Y$$

- Associated force

$$F_Y = \frac{1.6^3 \pi^3 R^2}{6} \left(\frac{\sigma_Y}{E^*} \right)^2 \sigma_Y$$

- Associated contact radius

$$a_Y = \frac{1.6\pi R}{2} \frac{\sigma_Y}{E^*}$$

- Plastic flow starts at the depth

$$z_Y \approx 1.21R \frac{\sigma_Y}{E^*}$$

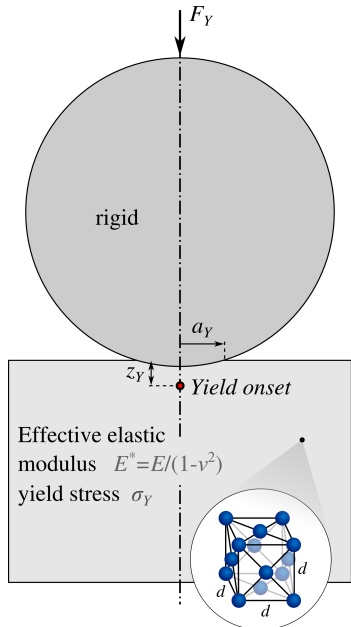
- Example: golden asperity

$$E^* \approx 96 \text{ GPa}, \quad \sigma_Y \approx 140 \text{ MPa}, \quad d \approx 4.1 \text{ \AA}$$

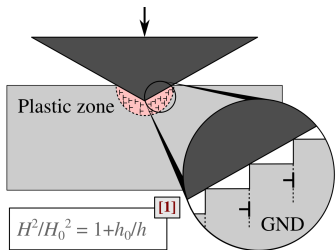
$$R = 1 \text{ } \mu\text{m}$$

$$F_Y \approx 38 \text{ nN}, \quad z_Y \approx 1.8 \text{ nm}, \quad a_Y \approx 3.6 \text{ nm}$$

$$z_Y \approx 4.5d, \quad a_Y \approx 11.5d$$

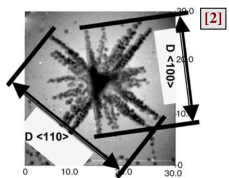
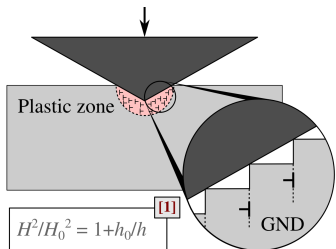


Indentation and hardness



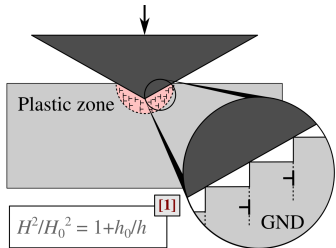
[1] Nix, Gao. *J Mech Phys Solids* (1998).

Indentation and hardness



- [1] Nix, Gao. *J Mech Phys Solids* (1998).
[2] Feng, Nix. *Scripta Mater* (2004).

Indentation and hardness



$$\frac{\text{Plastic zone } r}{\text{Contact radius } a} \sim 1 + b \exp(-h/h_1)$$

$$H^2/H_0^2 = 1 + [1 + b \exp(-h/h_1)]^{-3} h_0/h \quad [2]$$

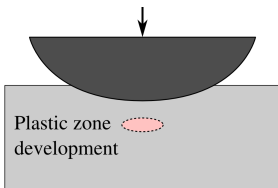
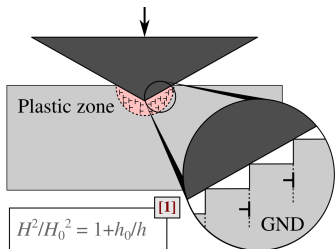
$$(H - H_p)^2 / (H_0 - H_p)^2 = 1 + [1 + b \exp(-h/h_1)]^{-3} h_0/h \quad [2,3]$$

[1] Nix, Gao. *J Mech Phys Solids* (1998).

[2] Feng, Nix. *Scripta Mater* (2004).

[3] Qui, Huang, Nix, Hwang, Gao. *Acta Mater* (2001).

Indentation and hardness



$$\frac{\text{Plastic zone } r}{\text{Contact radius } a} \sim 1 + b \exp(-h/h_1)$$

$$H^2/H_0^2 = 1 + [1 + b \exp(-h/h_1)]^{-3} h_0/h \quad [2]$$

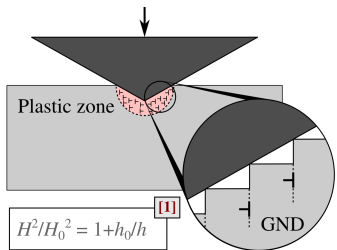
$$(H - H_p)^2 / (H_0 - H_p)^2 = 1 + [1 + b \exp(-h/h_1)]^{-3} h_0/h \quad [2,3]$$

[1] Nix, Gao. *J Mech Phys Solids* (1998).

[2] Feng, Nix. *Scripta Mater* (2004).

[3] Qui, Huang, Nix, Hwang, Gao. *Acta Mater* (2001).

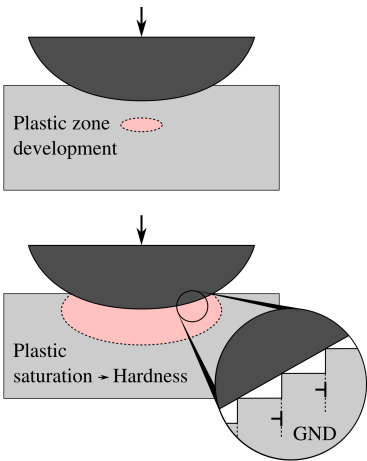
Indentation and hardness



$$\frac{\text{Plastic zone } r}{\text{Contact radius } a} \sim 1 + b \exp(-h/h_1)$$

$$H^2/H_0^2 = 1 + [1 + b \exp(-h/h_1)]^{-3} h_0/h \quad [2]$$

$$(H-H_p)^2/(H_0-H_p)^2 = 1 + [1 + b \exp(-h/h_1)]^{-3} h_0/h \quad [2,3]$$

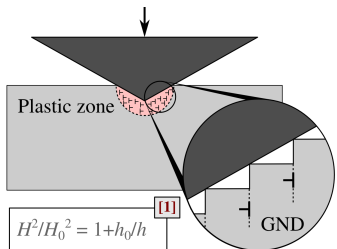


[1] Nix, Gao. *J Mech Phys Solids* (1998).

[2] Feng, Nix. *Scripta Mater* (2004).

[3] Qui, Huang, Nix, Hwang, Gao. *Acta Mater* (2001).

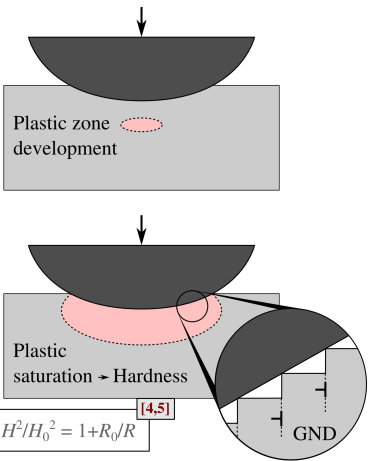
Indentation and hardness



$$\frac{\text{Plastic zone } r}{\text{Contact radius } a} \sim 1 + b \exp(-h/h_1)$$

$$H^2/H_0^2 = 1 + [1 + b \exp(-h/h_1)]^{-3} h_0/h \quad [2]$$

$$(H-H_p)^2/(H_0-H_p)^2 = 1 + [1 + b \exp(-h/h_1)]^{-3} h_0/h \quad [2,3]$$



[1] Nix, Gao. *J Mech Phys Solids* (1998).

[2] Feng, Nix. *Scripta Mater* (2004).

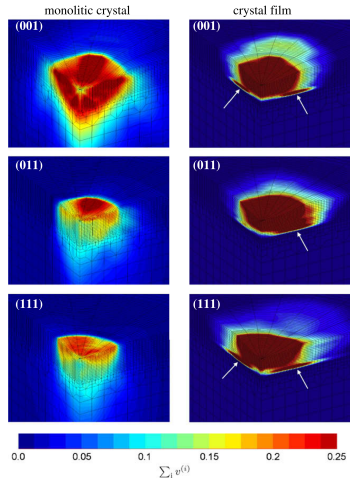
[3] Qui, Huang, Nix, Hwang, Gao. *Acta Mater* (2001).

[4] Swadener, George, Pharr. *J Mech Phys Solids* (2002).

[5] Gao, Larson, Lee, Nicola, Tischler, Pharr. *J Appl Mech* (2015).

Enhanced material behavior: beyond J_2 plasticity

- Crystal plasticity models
in indentation all slip systems are activated
Difference with isotropic plasticity is small
- Discrete models with inherent characteristic length
 - Molecular Dynamics
 - Dislocation Dynamics
- Continuum models with characteristic length
 - Cosserat continuum^[1]
 - Second-gradient plasticity^[2]



[1] Forest S., Sievert R. Elastoviscoplastic constitutive frameworks for generalized continua. *Acta Mech* 160 (2003)

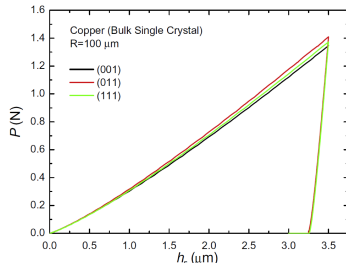
[2] Cordero N.M., Forest S. et al. Grain size effects on plastic strain and dislocation density tensor fields in metal polycrystals, *Comp Mater Sci* 52 (2012)

Spherical indentation of FCC copper crystal using crystal plasticity model in Zset

[3] Casals O., Forest S. Finite element crystal plasticity analysis of spherical indentation in bulk single crystals and coatings. *Comp Mater Sci* 45 (2009)

Enhanced material behavior: beyond J2 plasticity

- Crystal plasticity models
in indentation all slip systems are activated
Difference with isotropic plasticity is small
- Discrete models with inherent characteristic length
 - Molecular Dynamics
 - Dislocation Dynamics
- Continuum models with characteristic length
 - Cosserat continuum^[1]
 - Second-gradient plasticity^[2]



Spherical indentation of FCC copper crystal using crystal plasticity model in Zset

[3] Casals O., Forest S. Finite element crystal plasticity analysis of spherical indentation in bulk single crystals and coatings. *Comp Mater Sci* 45 (2009)

[1] Forest S., Sievert R. Elastoviscoplastic constitutive frameworks for generalized continua. *Acta Mech* 160 (2003)

[2] Cordero N.M., Forest S. et al. Grain size effects on plastic strain and dislocation density tensor fields in metal polycrystals, *Comp Mater Sci* 52 (2012)

Enhanced material behavior: beyond J2 plasticity

- Crystal plasticity models
in indentation all slip systems are activated

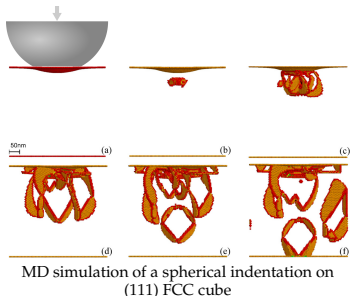
Difference with isotropic plasticity is small

- Discrete models with inherent characteristic length
 - Molecular Dynamics
 - Dislocation Dynamics

- Continuum models with characteristic length
 - Cosserat continuum^[1]
 - Second-gradient plasticity^[2]

[1] Forest S., Sievert R. Elastoviscoplastic constitutive frameworks for generalized continua. *Acta Mech* 160 (2003)

[2] Cordero N.M., Forest S. et al. Grain size effects on plastic strain and dislocation density tensor fields in metal polycrystals, *Comp Mater Sci* 52 (2012)



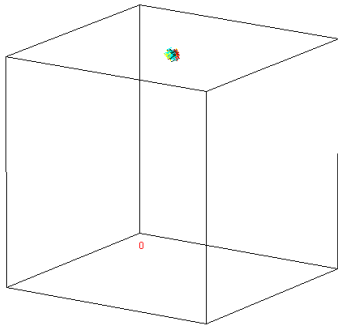
[4] H.J. Chang, M. Fivel, D. Rodney, M. Verdier. Multiscale modelling of indentation in FCC metals: From atomic to continuum, *CR Physique* 11 (2010)

Enhanced material behavior: beyond J2 plasticity

- Crystal plasticity models
in indentation all slip systems are activated
Difference with isotropic plasticity is small
- Discrete models with inherent characteristic length
 - Molecular Dynamics
 - Dislocation Dynamics
- Continuum models with characteristic length
 - Cosserat continuum^[1]
 - Second-gradient plasticity^[2]

[1] Forest S., Sievert R. Elastoviscoplastic constitutive frameworks for generalized continua. *Acta Mech* 160 (2003)

[2] Cordero N.M., Forest S. et al. Grain size effects on plastic strain and dislocation density tensor fields in metal polycrystals, *Comp Mater Sci* 52 (2012)



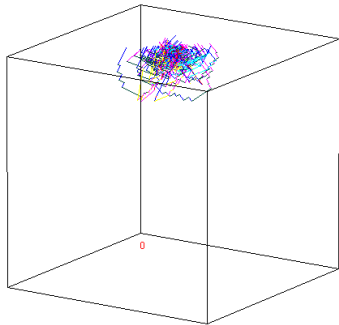
Resulting DD simulation of a spherical indentation on (111) FCC cube

[4] H.J. Chang, M. Fivel, D. Rodney, M. Verdier.
Multiscale modelling of indentation in FCC metals: From atomic to continuum, *CR Physique* 11 (2010)

www.numodis.com

Enhanced material behavior: beyond J2 plasticity

- Crystal plasticity models
in indentation all slip systems are activated
Difference with isotropic plasticity is small
- Discrete models with inherent characteristic length
 - Molecular Dynamics
 - Dislocation Dynamics
- Continuum models with characteristic length
 - Cosserat continuum^[1]
 - Second-gradient plasticity^[2]



Resulting DD simulation of a spherical indentation on (111) FCC cube

[4] H.J. Chang, M. Fivel, D. Rodney, M. Verdier.
Multiscale modelling of indentation in FCC metals: From atomic to continuum, CR Physique
11 (2010)

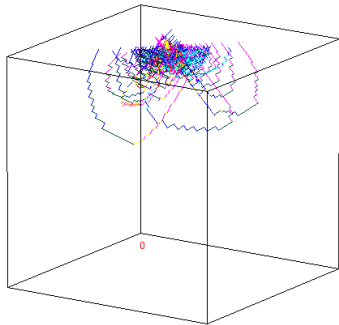
www.numodis.com

[1] Forest S., Sievert R. Elastoviscoplastic constitutive frameworks for generalized continua. *Acta Mech* 160 (2003)

[2] Cordero N.M., Forest S. et al. Grain size effects on plastic strain and dislocation density tensor fields in metal polycrystals, *Comp Mater Sci* 52 (2012)

Enhanced material behavior: beyond J2 plasticity

- Crystal plasticity models
in indentation all slip systems are activated
Difference with isotropic plasticity is small
- Discrete models with inherent characteristic length
 - Molecular Dynamics
 - Dislocation Dynamics
- Continuum models with characteristic length
 - Cosserat continuum^[1]
 - Second-gradient plasticity^[2]



Resulting DD simulation of a spherical indentation on (111) FCC cube

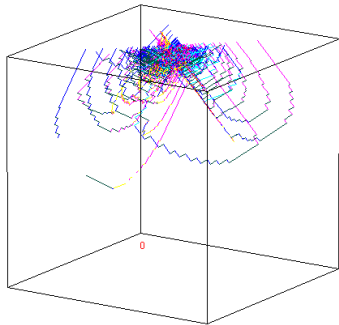
[4] H.J. Chang, M. Fivel, D. Rodney, M. Verdier.
Multiscale modelling of indentation in FCC metals: From atomic to continuum, CR Physique
11 (2010)
www.numodis.com

[1] Forest S., Sievert R. Elastoviscoplastic constitutive frameworks for generalized continua. *Acta Mech* 160 (2003)

[2] Cordero N.M., Forest S. et al. Grain size effects on plastic strain and dislocation density tensor fields in metal polycrystals, *Comp Mater Sci* 52 (2012)

Enhanced material behavior: beyond J2 plasticity

- Crystal plasticity models
in indentation all slip systems are activated
Difference with isotropic plasticity is small
- Discrete models with inherent characteristic length
 - Molecular Dynamics
 - Dislocation Dynamics
- Continuum models with characteristic length
 - Cosserat continuum^[1]
 - Second-gradient plasticity^[2]



Resulting DD simulation of a spherical indentation on (111) FCC cube

[4] H.J. Chang, M. Fivel, D. Rodney, M. Verdier.
Multiscale modelling of indentation in FCC metals: From atomic to continuum, CR Physique
11 (2010)
www.numodis.com

[1] Forest S., Sievert R. Elastoviscoplastic constitutive frameworks for generalized continua. *Acta Mech* 160 (2003)

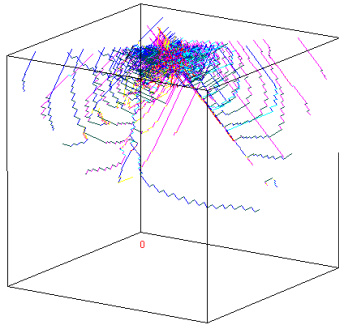
[2] Cordero N.M., Forest S. et al. Grain size effects on plastic strain and dislocation density tensor fields in metal polycrystals, *Comp Mater Sci* 52 (2012)

Enhanced material behavior: beyond J2 plasticity

- Crystal plasticity models
in indentation all slip systems are activated
Difference with isotropic plasticity is small
- Discrete models with inherent characteristic length
 - Molecular Dynamics
 - Dislocation Dynamics
- Continuum models with characteristic length
 - Cosserat continuum^[1]
 - Second-gradient plasticity^[2]

[1] Forest S., Sievert R. Elastoviscoplastic constitutive frameworks for generalized continua. *Acta Mech* 160 (2003)

[2] Cordero N.M., Forest S. et al. Grain size effects on plastic strain and dislocation density tensor fields in metal polycrystals, *Comp Mater Sci* 52 (2012)

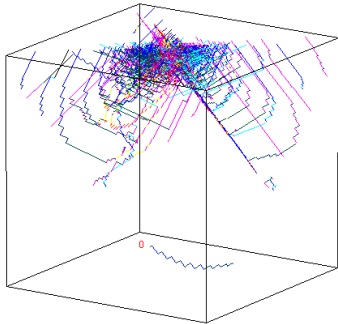


Resulting DD simulation of a spherical indentation on (111) FCC cube

[4] H.J. Chang, M. Fivel, D. Rodney, M. Verdier.
Multiscale modelling of indentation in FCC metals: From atomic to continuum, *CR Physique* 11 (2010)
www.numodis.com

Enhanced material behavior: beyond J2 plasticity

- Crystal plasticity models
in indentation all slip systems are activated
Difference with isotropic plasticity is small
- Discrete models with inherent characteristic length
 - Molecular Dynamics
 - Dislocation Dynamics
- Continuum models with characteristic length
 - Cosserat continuum^[1]
 - Second-gradient plasticity^[2]



Resulting DD simulation of a spherical indentation on (111) FCC cube

[4] H.J. Chang, M. Fivel, D. Rodney, M. Verdier.
Multiscale modelling of indentation in FCC metals: From atomic to continuum, CR Physique
11 (2010)

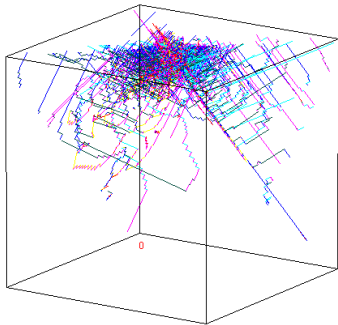
www.numodis.com

[1] Forest S., Sievert R. Elastoviscoplastic constitutive frameworks for generalized continua. *Acta Mech* 160 (2003)

[2] Cordero N.M., Forest S. et al. Grain size effects on plastic strain and dislocation density tensor fields in metal polycrystals, *Comp Mater Sci* 52 (2012)

Enhanced material behavior: beyond J2 plasticity

- Crystal plasticity models
in indentation all slip systems are activated
Difference with isotropic plasticity is small
- Discrete models with inherent characteristic length
 - Molecular Dynamics
 - Dislocation Dynamics
- Continuum models with characteristic length
 - Cosserat continuum^[1]
 - Second-gradient plasticity^[2]



Resulting DD simulation of a spherical indentation on (111) FCC cube

- [4] H.J. Chang, M. Fivel, D. Rodney, M. Verdier.
Multiscale modelling of indentation in FCC metals: From atomic to continuum, CR Physique
11 (2010)
www.numodis.com

[1] Forest S., Sievert R. Elastoviscoplastic constitutive frameworks for generalized continua. *Acta Mech* 160 (2003)

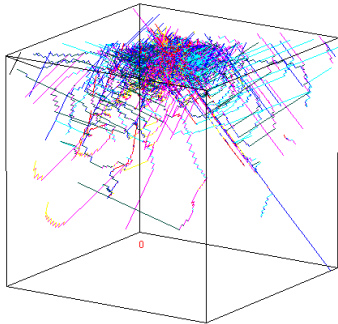
[2] Cordero N.M., Forest S. et al. Grain size effects on plastic strain and dislocation density tensor fields in metal polycrystals, *Comp Mater Sci* 52 (2012)

Enhanced material behavior: beyond J2 plasticity

- Crystal plasticity models
in indentation all slip systems are activated
Difference with isotropic plasticity is small
- Discrete models with inherent characteristic length
 - Molecular Dynamics
 - Dislocation Dynamics
- Continuum models with characteristic length
 - Cosserat continuum^[1]
 - Second-gradient plasticity^[2]

[1] Forest S., Sievert R. Elastoviscoplastic constitutive frameworks for generalized continua. *Acta Mech* 160 (2003)

[2] Cordero N.M., Forest S. et al. Grain size effects on plastic strain and dislocation density tensor fields in metal polycrystals, *Comp Mater Sci* 52 (2012)



Resulting DD simulation of a spherical indentation on (111) FCC cube

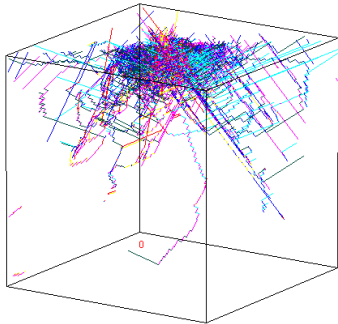
[4] H.J. Chang, M. Fivel, D. Rodney, M. Verdier.
Multiscale modelling of indentation in FCC metals: From atomic to continuum, *CR Physique* 11 (2010)
www.numodis.com

Enhanced material behavior: beyond J2 plasticity

- Crystal plasticity models
in indentation all slip systems are activated
Difference with isotropic plasticity is small
- Discrete models with inherent characteristic length
 - Molecular Dynamics
 - Dislocation Dynamics
- Continuum models with characteristic length
 - Cosserat continuum^[1]
 - Second-gradient plasticity^[2]

[1] Forest S., Sievert R. Elastoviscoplastic constitutive frameworks for generalized continua. *Acta Mech* 160 (2003)

[2] Cordero N.M., Forest S. et al. Grain size effects on plastic strain and dislocation density tensor fields in metal polycrystals, *Comp Mater Sci* 52 (2012)

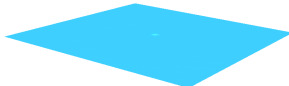


Resulting DD simulation of a spherical indentation on (111) FCC cube

[4] H.J. Chang, M. Fivel, D. Rodney, M. Verdier.
Multiscale modelling of indentation in FCC metals: From atomic to continuum, *CR Physique* 11 (2010)
www.numodis.com

Enhanced material behavior: beyond J_2 plasticity

- Crystal plasticity models
in indentation all slip systems are activated
Difference with isotropic plasticity is small
- Discrete models with inherent characteristic length
 - Molecular Dynamics
 - Dislocation Dynamics
- Continuum models with characteristic length
 - Cosserat continuum^[1]
 - Second-gradient plasticity^[2]



DD simulation of Berkovich nanoindentation

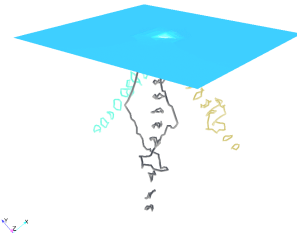
www.numodis.com

[1] Forest S., Sievert R. Elastoviscoplastic constitutive frameworks for generalized continua. *Acta Mech* 160 (2003)

[2] Cordero N.M., Forest S. et al. Grain size effects on plastic strain and dislocation density tensor fields in metal polycrystals, *Comp Mater Sci* 52 (2012)

Enhanced material behavior: beyond J_2 plasticity

- Crystal plasticity models
in indentation all slip systems are activated
Difference with isotropic plasticity is small
- Discrete models with inherent characteristic length
 - Molecular Dynamics
 - Dislocation Dynamics
- Continuum models with characteristic length
 - Cosserat continuum^[1]
 - Second-gradient plasticity^[2]



DD simulation of Berkovich nanoindentation

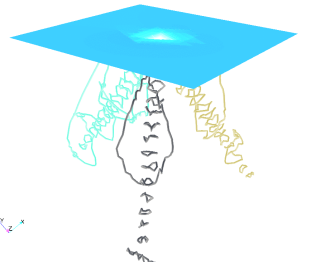
www.numodis.com

[1] Forest S., Sievert R. Elastoviscoplastic constitutive frameworks for generalized continua. *Acta Mech* 160 (2003)

[2] Cordero N.M., Forest S. et al. Grain size effects on plastic strain and dislocation density tensor fields in metal polycrystals, *Comp Mater Sci* 52 (2012)

Enhanced material behavior: beyond J_2 plasticity

- Crystal plasticity models
in indentation all slip systems are activated
Difference with isotropic plasticity is small
- Discrete models with inherent characteristic length
 - Molecular Dynamics
 - Dislocation Dynamics
- Continuum models with characteristic length
 - Cosserat continuum^[1]
 - Second-gradient plasticity^[2]



DD simulation of Berkovich nanoindentation

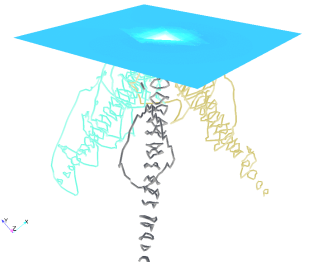
www.numodis.com

[1] Forest S., Sievert R. Elastoviscoplastic constitutive frameworks for generalized continua. *Acta Mech* 160 (2003)

[2] Cordero N.M., Forest S. et al. Grain size effects on plastic strain and dislocation density tensor fields in metal polycrystals, *Comp Mater Sci* 52 (2012)

Enhanced material behavior: beyond J_2 plasticity

- Crystal plasticity models
in indentation all slip systems are activated
Difference with isotropic plasticity is small
- Discrete models with inherent characteristic length
 - Molecular Dynamics
 - Dislocation Dynamics
- Continuum models with characteristic length
 - Cosserat continuum^[1]
 - Second-gradient plasticity^[2]



DD simulation of Berkovich nanoindentation

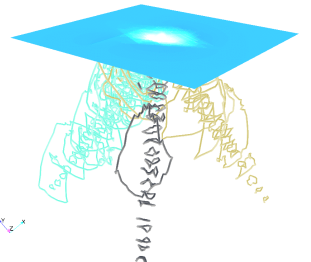
www.numodis.com

[1] Forest S., Sievert R. Elastoviscoplastic constitutive frameworks for generalized continua. *Acta Mech* 160 (2003)

[2] Cordero N.M., Forest S. et al. Grain size effects on plastic strain and dislocation density tensor fields in metal polycrystals, *Comp Mater Sci* 52 (2012)

Enhanced material behavior: beyond J_2 plasticity

- Crystal plasticity models
in indentation all slip systems are activated
Difference with isotropic plasticity is small
- Discrete models with inherent characteristic length
 - Molecular Dynamics
 - Dislocation Dynamics
- Continuum models with characteristic length
 - Cosserat continuum^[1]
 - Second-gradient plasticity^[2]



DD simulation of Berkovich nanoindentation

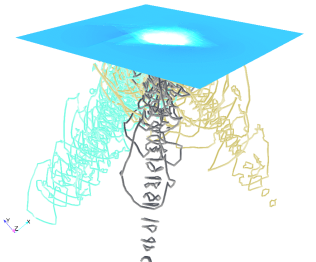
www.numodis.com

[1] Forest S., Sievert R. Elastoviscoplastic constitutive frameworks for generalized continua. *Acta Mech* 160 (2003)

[2] Cordero N.M., Forest S. et al. Grain size effects on plastic strain and dislocation density tensor fields in metal polycrystals, *Comp Mater Sci* 52 (2012)

Enhanced material behavior: beyond J_2 plasticity

- Crystal plasticity models
in indentation all slip systems are activated
Difference with isotropic plasticity is small
- Discrete models with inherent characteristic length
 - Molecular Dynamics
 - Dislocation Dynamics
- Continuum models with characteristic length
 - Cosserat continuum^[1]
 - Second-gradient plasticity^[2]



DD simulation of Berkovich nanoindentation

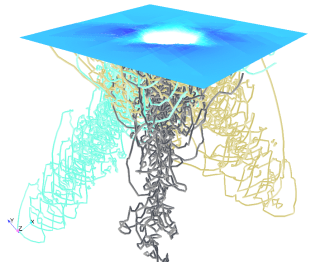
www.numodis.com

[1] Forest S., Sievert R. Elastoviscoplastic constitutive frameworks for generalized continua. *Acta Mech* 160 (2003)

[2] Cordero N.M., Forest S. et al. Grain size effects on plastic strain and dislocation density tensor fields in metal polycrystals, *Comp Mater Sci* 52 (2012)

Enhanced material behavior: beyond J_2 plasticity

- Crystal plasticity models
in indentation all slip systems are activated
Difference with isotropic plasticity is small
- Discrete models with inherent characteristic length
 - Molecular Dynamics
 - Dislocation Dynamics
- Continuum models with characteristic length
 - Cosserat continuum^[1]
 - Second-gradient plasticity^[2]



DD simulation of Berkovich nanoindentation

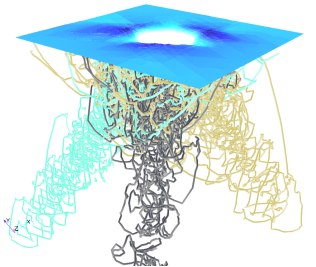
www.numodis.com

[1] Forest S., Sievert R. Elastoviscoplastic constitutive frameworks for generalized continua. *Acta Mech* 160 (2003)

[2] Cordero N.M., Forest S. et al. Grain size effects on plastic strain and dislocation density tensor fields in metal polycrystals, *Comp Mater Sci* 52 (2012)

Enhanced material behavior: beyond J_2 plasticity

- Crystal plasticity models
in indentation all slip systems are activated
Difference with isotropic plasticity is small
- Discrete models with inherent characteristic length
 - Molecular Dynamics
 - Dislocation Dynamics
- Continuum models with characteristic length
 - Cosserat continuum^[1]
 - Second-gradient plasticity^[2]



DD simulation of Berkovich nanoindentation

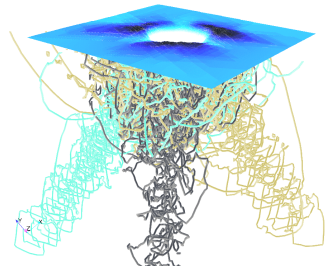
www.numodis.com

[1] Forest S., Sievert R. Elastoviscoplastic constitutive frameworks for generalized continua. *Acta Mech* 160 (2003)

[2] Cordero N.M., Forest S. et al. Grain size effects on plastic strain and dislocation density tensor fields in metal polycrystals, *Comp Mater Sci* 52 (2012)

Enhanced material behavior: beyond J_2 plasticity

- Crystal plasticity models
in indentation all slip systems are activated
Difference with isotropic plasticity is small
- Discrete models with inherent characteristic length
 - Molecular Dynamics
 - Dislocation Dynamics
- Continuum models with characteristic length
 - Cosserat continuum^[1]
 - Second-gradient plasticity^[2]



DD simulation of Berkovich nanoindentation

www.numodis.com

[1] Forest S., Sievert R. Elastoviscoplastic constitutive frameworks for generalized continua. *Acta Mech* 160 (2003)

[2] Cordero N.M., Forest S. et al. Grain size effects on plastic strain and dislocation density tensor fields in metal polycrystals, *Comp Mater Sci* 52 (2012)

Cosserat continuum

- Field variables (displacement & rotation): $\underline{u}, \underline{\omega}$
- Small deformation tensor: $\underline{\underline{\epsilon}} = \nabla \underline{u} + {}^3\underline{\epsilon} \cdot \underline{\omega}$
- Torsion-curvature tensor: $\underline{\underline{\kappa}} = \nabla \underline{\omega}$
- Elasticity: $\underline{\sigma} = \lambda \text{tr}(\underline{\underline{\epsilon}}) \underline{I} + \mu(\underline{\underline{\epsilon}} + \underline{\underline{\epsilon}}^\top) + \mu_c(\underline{\underline{\epsilon}} - \underline{\underline{\epsilon}}^\top), \quad \underline{m} = \alpha \text{tr}(\underline{\underline{\kappa}}) \underline{I} + 2\beta \underline{\underline{\kappa}}$

$$l_e = \sqrt{\beta/\mu}$$

Note: $\underline{\underline{\epsilon}}^\top \neq \underline{\underline{\epsilon}}, \underline{\underline{\kappa}}^\top \neq \underline{\underline{\kappa}}, \underline{\sigma}^\top \neq \underline{\sigma}, \underline{m}^\top \neq \underline{m}$

- In non-inertial problems without volume forces and couple-forces, balance of momentum and of moment of momentum:

$$\nabla \cdot \underline{\sigma} = 0, \quad \nabla \cdot \underline{m} - {}^3\underline{\epsilon} : \underline{\sigma} = 0$$

- Plasticity: equivalent stress^[1,2] $Y = \sqrt{\frac{3}{2} \left(a_1 \underline{s} : \underline{s} + a_2 \underline{s} : \underline{s}^\top + \left[\frac{1}{l_p^2} \right] \underline{m} : \underline{m} \right)}$
- Internal lengths: elastic l_e , plastic l_p

[1] R. de Borst, L.J. Sluys, *Comp Meth Appl Mech Engin* (1991)

[2] S. Forest, R. Sievert, *Acta Mech* (2003)

where permutation tensor ${}^3\underline{\epsilon} \sim \epsilon_{ijk} = \begin{cases} 1, & \text{if } \{ijk\} = \{123\} \text{ or } \{231\} \text{ or } \{312\} \\ -1, & \text{if } \{ijk\} = \{321\} \text{ or } \{213\} \text{ or } \{132\} \\ 0, & \text{otherwise} \end{cases}$

Single asperity analysis

Assumptions

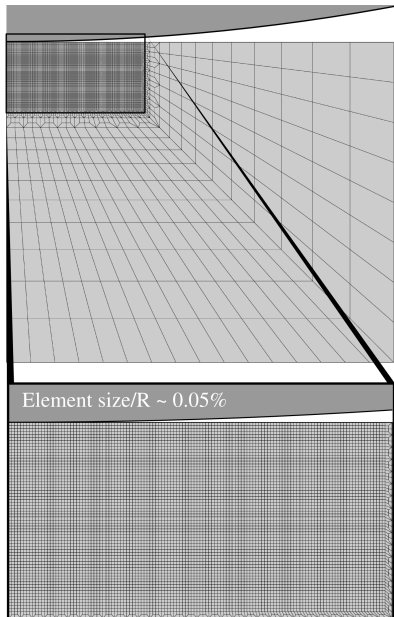
- Rigid spherical asperity
- Axisymmetric FE problem
- Generalized Cosserat continuum

Parameters

- Au: $E = 96 \text{ GPa}$, $\nu = 0.42$,
 $\sigma_y = 140 \text{ MPa}$
- $\mu_c = 10\mu$, $l_e = 100 \text{ nm}$, $a_1 = 1$
- Indenter radius
 $R \in [0.002, 2000] \mu\text{m}$

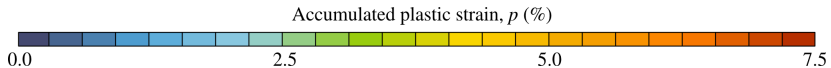
Objectives

- Study size effect
- Enhance asperity based models
for rough contact



Accumulated plasticity

- Different plastic distribution



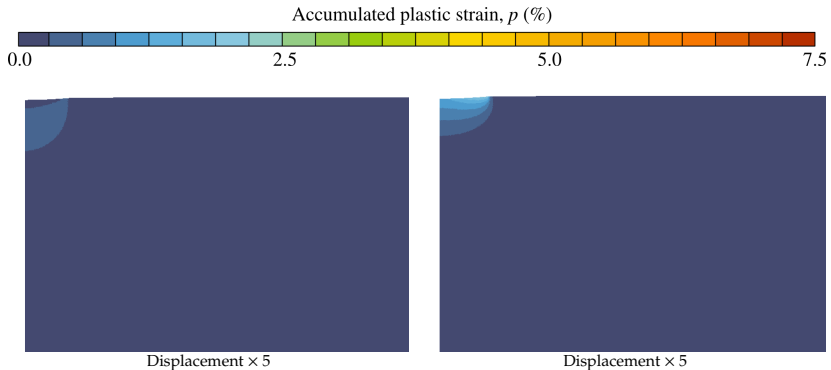
Indenter radius $R = 20\mu\text{m}$
Max plastic strain $p_{\max} \approx 7.5\%$



Indenter radius $R = 2\mu\text{m}$
Max plastic strain $p_{\max} \approx 11\%$

Accumulated plasticity

- Different plastic distribution

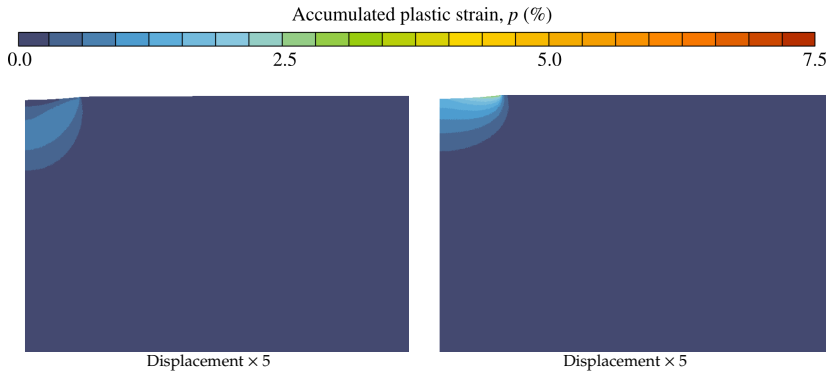


Indenter radius $R = 20\mu\text{m}$
Max plastic strain $p_{\max} \approx 7.5\%$

Indenter radius $R = 2\mu\text{m}$
Max plastic strain $p_{\max} \approx 11\%$

Accumulated plasticity

- Different plastic distribution

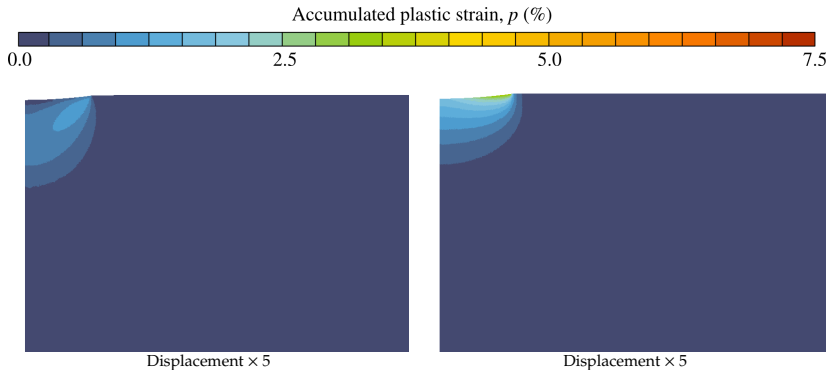


Indenter radius $R = 20\mu\text{m}$
Max plastic strain $p_{\max} \approx 7.5\%$

Indenter radius $R = 2\mu\text{m}$
Max plastic strain $p_{\max} \approx 11\%$

Accumulated plasticity

- Different plastic distribution

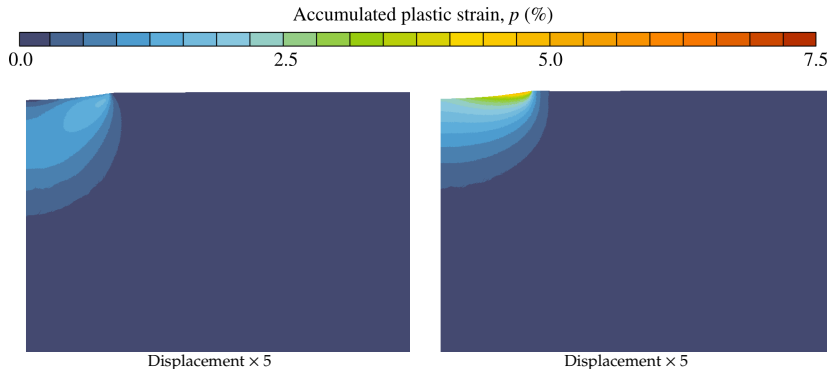


Indenter radius $R = 20\mu\text{m}$
Max plastic strain $p_{\max} \approx 7.5\%$

Indenter radius $R = 2\mu\text{m}$
Max plastic strain $p_{\max} \approx 11\%$

Accumulated plasticity

- Different plastic distribution

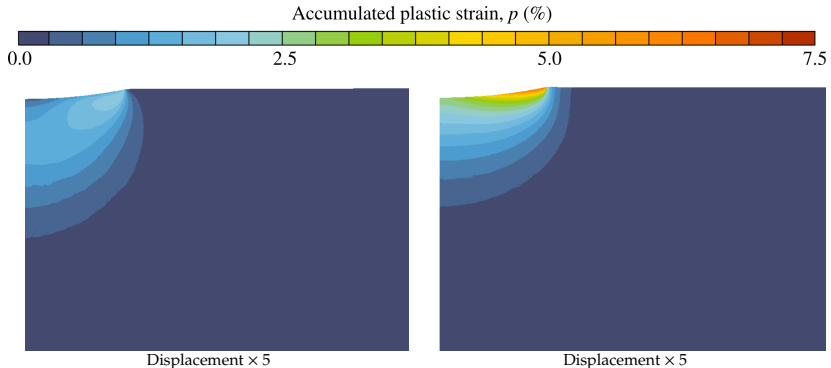


Indenter radius $R = 20\mu\text{m}$
Max plastic strain $p_{\max} \approx 7.5\%$

Indenter radius $R = 2\mu\text{m}$
Max plastic strain $p_{\max} \approx 11\%$

Accumulated plasticity

- Different plastic distribution

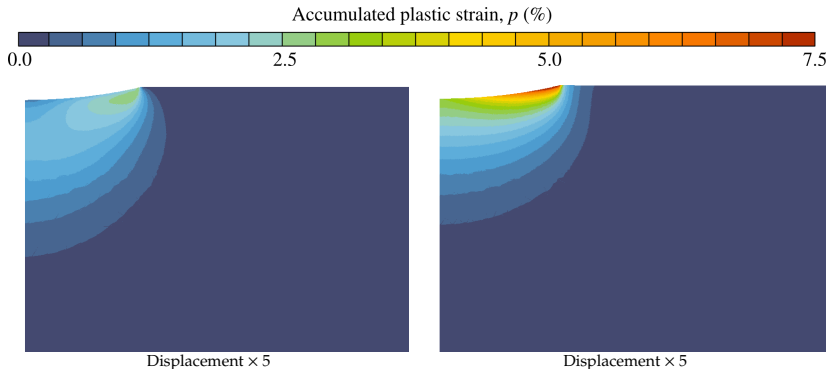


Indenter radius $R = 20\mu\text{m}$
Max plastic strain $p_{\max} \approx 7.5\%$

Indenter radius $R = 2\mu\text{m}$
Max plastic strain $p_{\max} \approx 11\%$

Accumulated plasticity

- Different plastic distribution

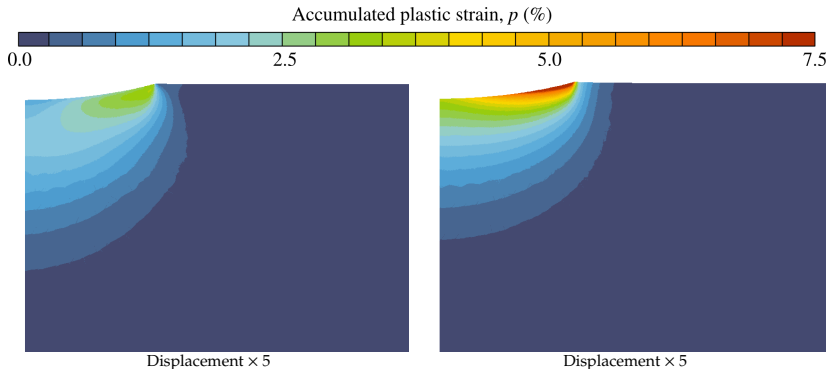


Indenter radius $R = 20\mu\text{m}$
Max plastic strain $p_{\max} \approx 7.5\%$

Indenter radius $R = 2\mu\text{m}$
Max plastic strain $p_{\max} \approx 11\%$

Accumulated plasticity

- Different plastic distribution

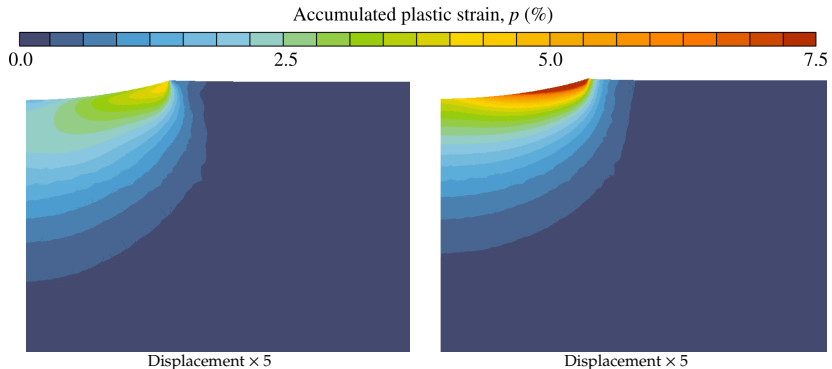


Indenter radius $R = 20\mu\text{m}$
Max plastic strain $p_{\max} \approx 7.5\%$

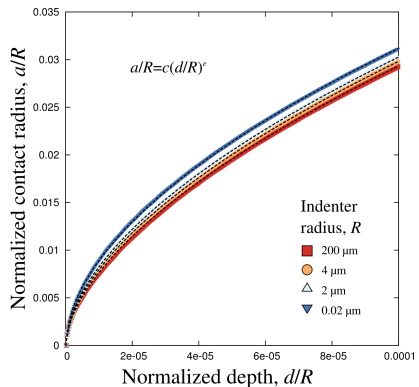
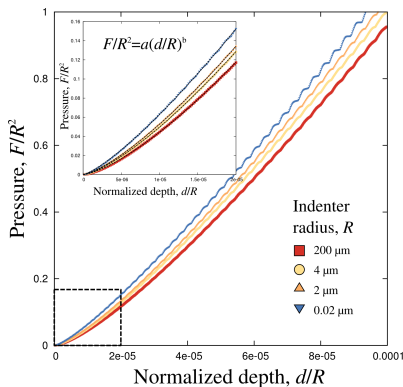
Indenter radius $R = 2\mu\text{m}$
Max plastic strain $p_{\max} \approx 11\%$

Accumulated plasticity

- Different plastic distribution



Displacement–force–contact radius

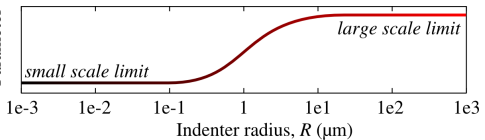


Parameters:

$$a(R), b(R), c(R), e(R)$$

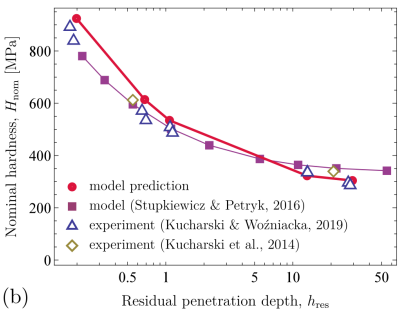
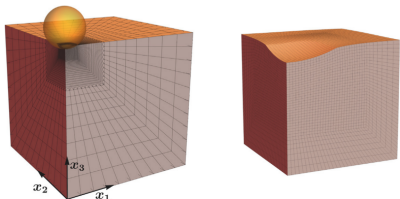
else: using NURBS curve fit.

Parameter



Working model

- Gradient-enhanced hardening with the Cosserat crystal plasticity theory^[1]
- Cubic elasticity with C_{11}, C_{12}, C_{44} is to be taken into account

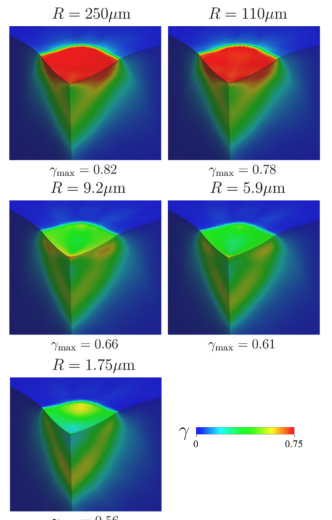


[1] Ryś, M., Stupkiewicz, S. and Petryk, H., 2022. Micropolar regularization of crystal plasticity with the gradient-enhanced incremental hardening law. International Journal of Plasticity, 156, p.103355.

Working model

- Gradient-enhanced hardening with the Cosserat crystal plasticity theory^[1]
- Cubic elasticity with C_{11}, C_{12}, C_{44} is to be taken into account

[1] Ryś, M., Stupkiewicz, S. and Petryk, H., 2022. Micropolar regularization of crystal plasticity with the gradient-enhanced incremental hardening law. International Journal of Plasticity, 156, p.103355.



Residual plastic slip for different indenter radii R

Viscoelasticity

Viscoelastic material

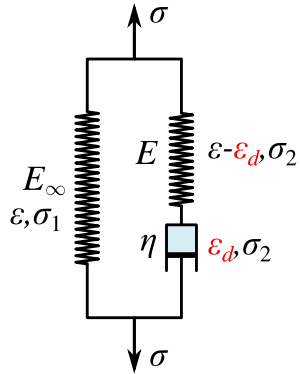
One-dimensional constitutive equations

- Applied stress σ
- In the left branch $\sigma_1 = E_\infty \varepsilon$
- In the dashpot $\sigma_2 = \eta \dot{\varepsilon}_d$ (*)
- In the right spring $\sigma_2 = E(\varepsilon - \varepsilon_d)$ (**)
- For the whole system $\sigma = \sigma_1 + \sigma_2$

$$\boxed{\sigma = (E_\infty + E)\varepsilon - E\varepsilon_d}$$

- From (*) and (**), and denoting $\tau = \eta/E$:

$$\boxed{\dot{\varepsilon}_d + \frac{\varepsilon_d}{\tau} = \frac{\varepsilon}{\tau}, \quad \varepsilon_d \xrightarrow{t \rightarrow -\infty} 0}$$



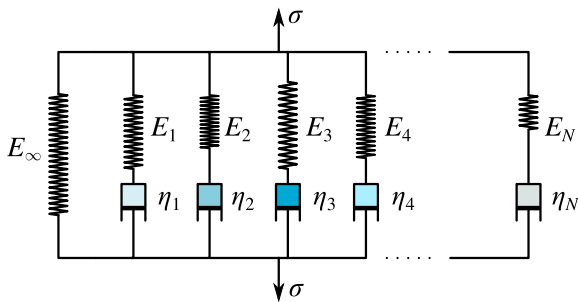
• One-dimensional viscoelastic model

- Recall: 1D model

$$\sigma = (E_\infty + E)\varepsilon - E\varepsilon_d, \quad \dot{\varepsilon}_d + \frac{\varepsilon_d}{\tau} = \frac{\varepsilon}{\tau}, \quad \varepsilon_d \xrightarrow[t \rightarrow -\infty]{} 0$$

- Multiple dashpots in parallel

$$\underbrace{\sigma = (E_\infty + \sum_i E_i)\varepsilon - \sum_i E_i \varepsilon_d^i}_{\text{elastic stress } \sigma_0}, \quad \dot{\varepsilon}_d^i + \frac{\varepsilon_d^i}{\tau_i} = \frac{\varepsilon}{\tau_i}, \quad \varepsilon_d^i \xrightarrow[t \rightarrow -\infty]{} 0, \quad \tau_i = \frac{\eta_i}{E_i}$$



• One-dimensional viscoelastic model

- Recall: 1D model

$$\sigma = (E_\infty + E)\varepsilon - E\varepsilon_d, \quad \dot{\varepsilon}_d + \frac{\varepsilon_d}{\tau} = \frac{\varepsilon}{\tau}, \quad \varepsilon_d \xrightarrow[t \rightarrow -\infty]{} 0$$

- Multiple dashpots in parallel

$$\sigma = (\underbrace{E_\infty + \sum_i E_i}_{\text{elastic stress } \sigma_0})\varepsilon - \sum_i E_i \varepsilon_d^i, \quad \dot{\varepsilon}_d^i + \frac{\varepsilon_d^i}{\tau_i} = \frac{\varepsilon}{\tau_i}, \quad \varepsilon_d^i \xrightarrow[t \rightarrow -\infty]{} 0, \quad \tau_i = \frac{\eta_i}{E_i}$$

- Denote $E_0 = E_\infty + \sum_i E_i$, $\psi_i = E_i/E_0$, and $q_i = E_i \varepsilon_d^i$ we obtain

$$\sigma = E_0 \varepsilon - \sum_i q_i, \quad \dot{q}_i + \frac{q_i}{\tau_i} = \frac{\psi_i}{\tau_i} \sigma_0, \quad \varepsilon_d^i \xrightarrow[t \rightarrow -\infty]{} 0$$

- By construction

$$\sum_i \psi_i + \frac{E_\infty}{E_0} = 1 \quad \Rightarrow \quad \sum_i \psi_i = 1 - \frac{E_\infty}{E_0}$$

• Three-dimensional viscoelastic model

Linear viscoelastic (generalized Maxwell model, standard solid)

- Stress-strain relation:

$$\underline{\underline{\sigma}}(t) = K\theta \underline{\underline{I}} + \int_{-\infty}^t G(t-\tau) \dot{\underline{\underline{e}}}(\tau) d\tau,$$

- Kernel $G(\tau)$ is given by:

$$G(\tau) = 2G_\infty + 2(G_0 - G_\infty)\Psi(\tau) \text{ with } \Psi(\tau) = \sum_{i=1}^n \psi_i \exp(-\tau/\tau_i)$$

- G_∞, G_0 are the slow/fast loading shear moduli, respectively, such that $G_\infty \leq G_0$;
- K is the bulk modulus, and for elastomers/polymers $K/G_0 \gg 1$;
- ψ_i are the influence coefficients, such that $\sum_{i=1}^n \psi_i = 1$;
- τ_i are the respective relaxation times.

• Material model: *storage* and loss moduli

- Consider a harmonic (rigid) loading: $\underline{e}(t) = \underline{e}_0 \exp(i\omega t)$
- Split the kernel: $G(t) = 2G_\infty + \tilde{G}(t)$
- Then, the storage modulus (general case):

$$G'(\omega) = 2G_\infty + \omega \int_0^\infty \tilde{G}(\tau) \sin(\omega\tau) d\tau$$

- The storage modulus in the framework of the generalized Maxwell model:

$$G'(\omega) = 2G_\infty + 2\omega(G_0 - G_\infty) \sum_{i=1}^n \psi_i \int_0^\infty \exp(-\tau/\tau_i) \sin(\omega\tau) d\tau$$

$$G'(\omega) = 2G_\infty + 2(G_0 - G_\infty) \sum_{i=1}^n \frac{\psi_i \omega^2 \tau_i^2}{1 + \omega^2 \tau_i^2}$$

- Remark:

$$\int \exp(cx) \sin(bx) dx = \frac{\exp(cx)}{c^2 + b^2} [c \sin(bx) - b \cos(bx)]$$

- Material model: storage and loss moduli

- The loss modulus (general case):

$$G''(\omega) = \omega \int_0^{\infty} \tilde{G}(\tau) \cos(\omega\tau) d\tau$$

- The loss modulus in the framework of the generalized Maxwell model:

$$G''(\omega) = 2\omega(G_0 - G_{\infty}) \sum_{i=1}^n \psi_i \int_0^{\infty} \exp(-\tau/\tau_i) \cos(\omega\tau) d\tau$$

$$G''(\omega) = 2(G_0 - G_{\infty}) \sum_{i=1}^n \frac{\psi_i \omega \tau_i}{1 + \omega^2 \tau_i^2}.$$

- Remark:

$$\int \exp(cx) \cos(bx) dx = \frac{\exp(cx)}{c^2 + b^2} [c \cos(bx) + b \sin(bx)]$$

• Material model: example

- Material parameters: $G_0 = 1.1 \text{ MPa}$, $G_\infty = 50 \text{ kPa}$
- Single relaxation time: $\tau_0 = 10^{-7} \text{ s}$
- Quasi-incompressible material: $K/G_0 = 10^6 \gg 1$
- Uniaxial (rigid) loading: $\varepsilon_{xx} = A \sin(\omega t)$, $\sigma_{yy} = \sigma_{zz} = 0$, $\varepsilon_{yy} = \varepsilon_{zz} \approx -0.5\varepsilon_{xx}$
- Spherical and deviatoric parts: $\underline{\epsilon} \approx A(1 - 2\nu) \sin(\omega t) \underline{I}$, $\underline{e} \approx \underline{\epsilon}$
- Stress-strain relation:

$$\underline{\sigma}(t) = \int_{-\infty}^t 2(G_0 - G_\infty) \exp[-(t - \tau)/\tau_0] \dot{\underline{e}}(\tau) d\tau + 2G_\infty \underline{e} + K\underline{\epsilon},$$

- Axial and radial stress components:

$$\sigma_{xx} = 2G_\infty \varepsilon_{xx} + K(\varepsilon_{xx} + 2\varepsilon_{yy}) + \int_{-\infty}^t 2(G_0 - G_\infty) \exp[-(t - \tau)/\tau_0] \dot{\varepsilon}_{xx}(\tau) d\tau$$

• Material model: example

- Material parameters: $G_0 = 1.1 \text{ MPa}$, $G_\infty = 50 \text{ kPa}$
- Single relaxation time: $\tau_0 = 10^{-7} \text{ s}$
- Quasi-incompressible material: $K/G_0 = 10^6 \gg 1$
- Uniaxial (rigid) loading: $\varepsilon_{xx} = A \sin(\omega t)$, $\sigma_{yy} = \sigma_{zz} = 0$, $\varepsilon_{yy} = \varepsilon_{zz} \approx -0.5\varepsilon_{xx}$
- Spherical and deviatoric parts: $\underline{\epsilon} \approx A(1 - 2\nu) \sin(\omega t) \underline{I}$, $\underline{e} \approx \underline{\epsilon}$
- Stress-strain relation:

$$\underline{\sigma}(t) = \int_{-\infty}^t 2(G_0 - G_\infty) \exp[-(t - \tau)/\tau_0] \dot{\underline{e}}(\tau) d\tau + 2G_\infty \underline{e} + K\underline{\epsilon},$$

- Axial and radial stress components:

$$\sigma_{xx} = 2G_\infty \varepsilon_{xx} + K(\varepsilon_{xx} + 2\varepsilon_{yy}) + \int_{-\infty}^t 2(G_0 - G_\infty) \exp[-(t - \tau)/\tau_0] \dot{\varepsilon}_{xx}(\tau) d\tau$$

$$\sigma_{yy} = 0$$

• Material model: example

- Material parameters: $G_0 = 1.1 \text{ MPa}$, $G_\infty = 50 \text{ kPa}$
- Single relaxation time: $\tau_0 = 10^{-7} \text{ s}$
- Quasi-incompressible material: $K/G_0 = 10^6 \gg 1$
- Uniaxial (rigid) loading: $\varepsilon_{xx} = A \sin(\omega t)$, $\sigma_{yy} = \sigma_{zz} = 0$, $\varepsilon_{yy} = \varepsilon_{zz} \approx -0.5\varepsilon_{xx}$
- Spherical and deviatoric parts: $\underline{\epsilon} \approx A(1 - 2\nu) \sin(\omega t) \underline{I}$, $\underline{e} \approx \underline{\epsilon}$
- Stress-strain relation:

$$\underline{\sigma}(t) = \int_{-\infty}^t 2(G_0 - G_\infty) \exp[-(t - \tau)/\tau_0] \dot{\underline{\epsilon}}(\tau) d\tau + 2G_\infty \underline{e} + K\underline{\epsilon},$$

- Axial and radial stress components:

$$\sigma_{xx} = 2G_\infty \varepsilon_{xx} + K(\varepsilon_{xx} + 2\varepsilon_{yy}) + \int_{-\infty}^t 2(G_0 - G_\infty) \exp[-(t - \tau)/\tau_0] \dot{\varepsilon}_{xx}(\tau) d\tau$$

$$\sigma_{yy} = 0 = 2G_\infty \varepsilon_{yy} + K(\varepsilon_{xx} + 2\varepsilon_{yy}) + \int_{-\infty}^t 2(G_0 - G_\infty) \exp[-(t - \tau)/\tau_0] \dot{\varepsilon}_{yy}(\tau) d\tau$$

• Material model: example

- Material parameters: $G_0 = 1.1 \text{ MPa}$, $G_\infty = 50 \text{ kPa}$
- Single relaxation time: $\tau_0 = 10^{-7} \text{ s}$
- Quasi-incompressible material: $K/G_0 = 10^6 \gg 1$
- Uniaxial (rigid) loading: $\varepsilon_{xx} = A \sin(\omega t)$, $\sigma_{yy} = \sigma_{zz} = 0$, $\varepsilon_{yy} = \varepsilon_{zz} \approx -0.5\varepsilon_{xx}$
- Spherical and deviatoric parts: $\underline{\epsilon} \approx A(1 - 2\nu) \sin(\omega t) \underline{I}$, $\underline{e} \approx \underline{\epsilon}$
- Stress-strain relation:

$$\underline{\sigma}(t) = \int_{-\infty}^t 2(G_0 - G_\infty) \exp[-(t - \tau)/\tau_0] \dot{\underline{\epsilon}}(\tau) d\tau + 2G_\infty \underline{e} + K\underline{\epsilon},$$

- Axial and radial stress components:

$$\sigma_{xx} = 2G_\infty \varepsilon_{xx} + K(\varepsilon_{xx} + 2\varepsilon_{yy}) + \int_{-\infty}^t 2(G_0 - G_\infty) \exp[-(t - \tau)/\tau_0] \dot{\varepsilon}_{xx}(\tau) d\tau$$

$$\sigma_{yy} = 0 = 2G_\infty \varepsilon_{yy} + K(\varepsilon_{xx} + 2\varepsilon_{yy}) + \int_{-\infty}^t 2(G_0 - G_\infty) \exp[-(t - \tau)/\tau_0] \dot{\varepsilon}_{yy}(\tau) d\tau$$

$$\sigma_{xx} = 3G_\infty \varepsilon_{xx} + \int_{-\infty}^t 3(G_0 - G_\infty) \exp[-(t - \tau)/\tau_0] \dot{\varepsilon}_{xx}(\tau) d\tau$$

• Material model: example II

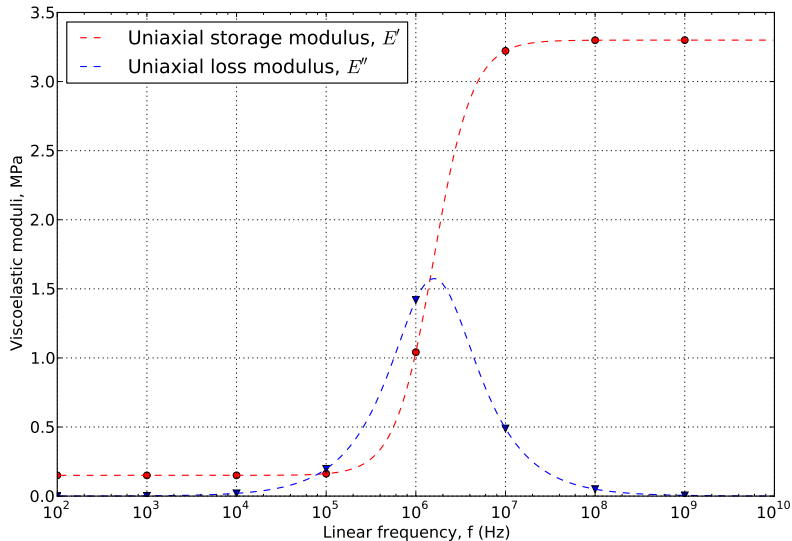
- Uniaxial storage modulus:

$$E'(\omega) = 3G_\infty + 3(G_0 - G_\infty) \frac{\omega^2 \tau_0^2}{1 + \omega^2 \tau_0^2}$$

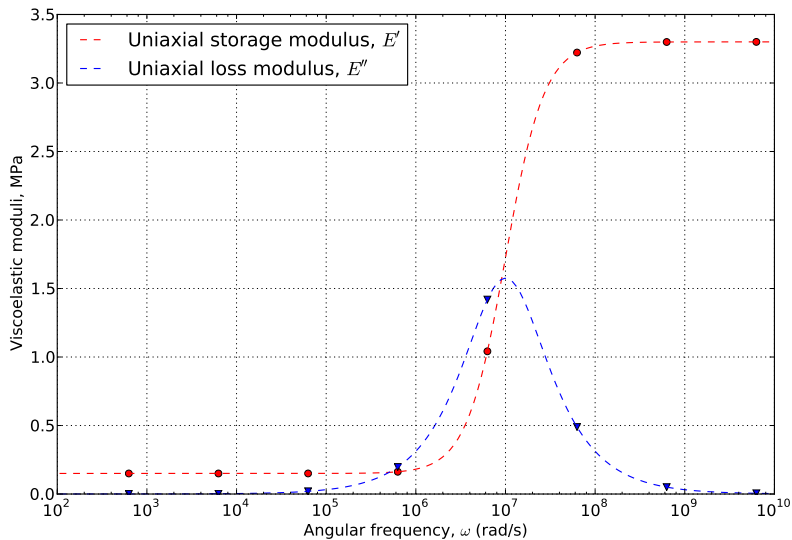
- Uniaxial loss modulus:

$$E''(\omega) = 3(G_0 - G_\infty) \frac{\omega \tau}{1 + \omega^2 \tau_0^2}$$

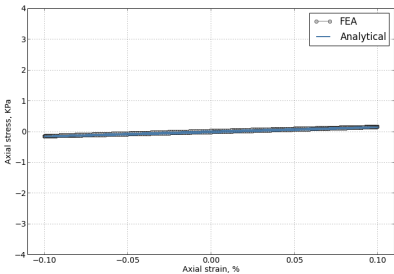
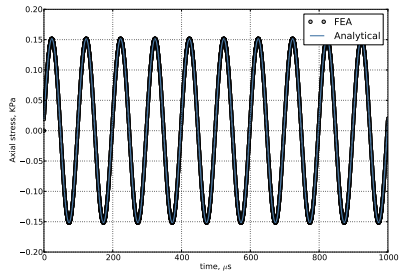
- Material model: example (FEA vs Analytics)



- Material model: example (FEA vs Analytics)

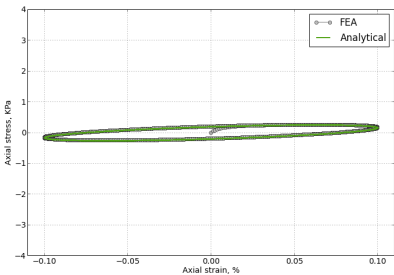
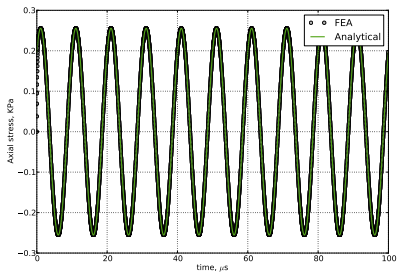


- Material model: example (FEA vs Analytics)



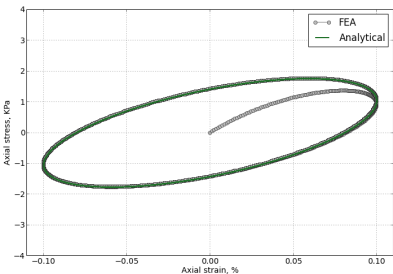
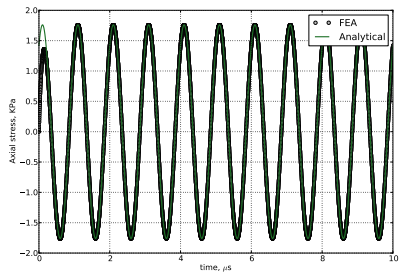
Linear frequency $f = 10^4$ Hz

- Material model: example (FEA vs Analytics)



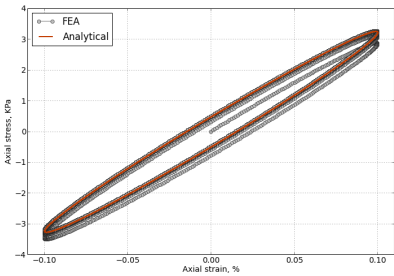
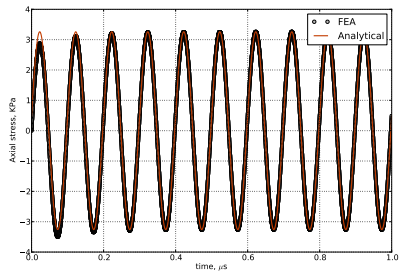
Linear frequency $f = 10^5$ Hz

- Material model: example (FEA vs Analytics)



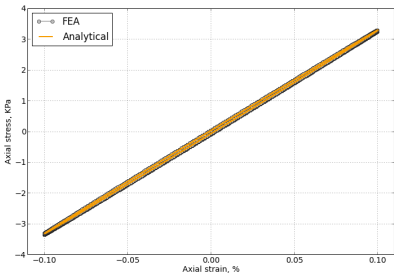
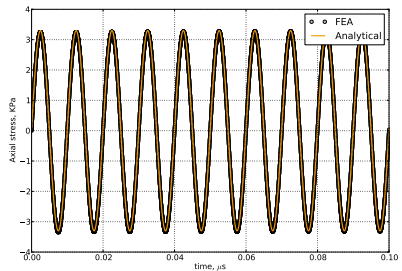
Linear frequency $f = 10^6$ Hz

- Material model: example (FEA vs Analytics)



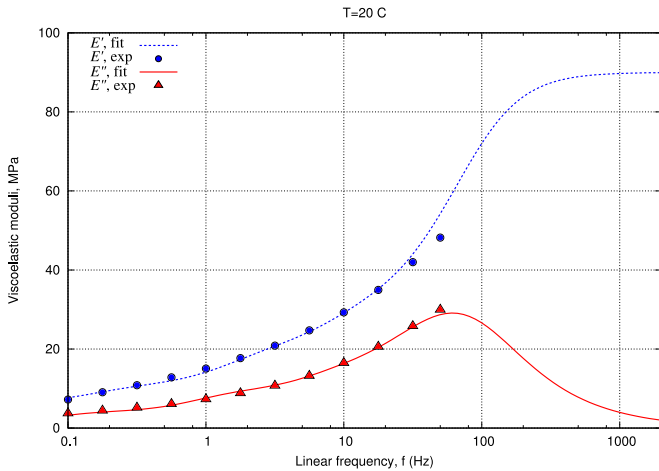
Linear frequency $f = 10^7$ Hz

- Material model: example (FEA vs Analytics)



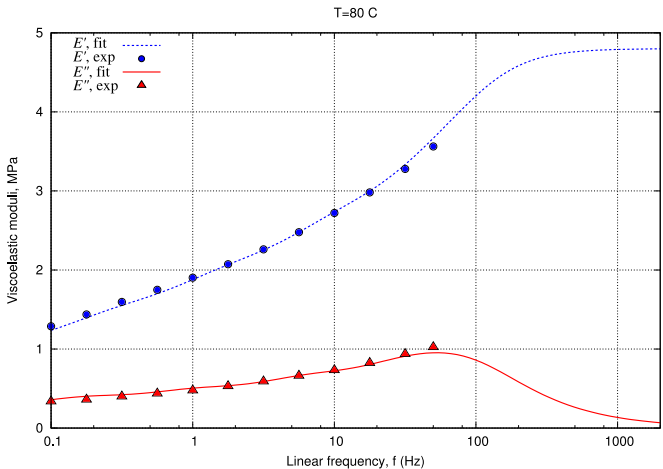
Linear frequency $f = 10^8$ Hz

Viscoelastic sliding: bulk friction



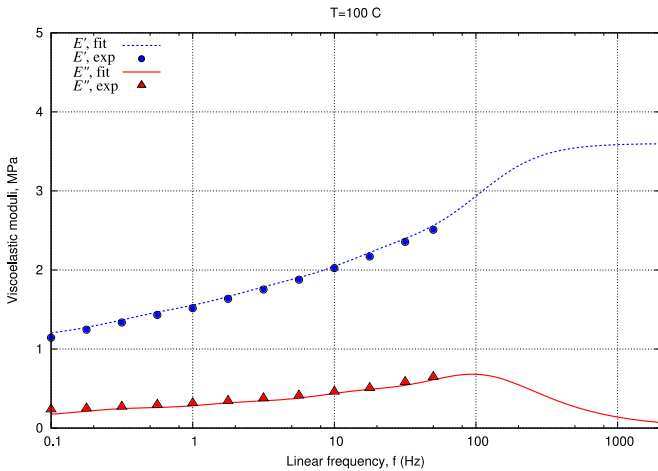
Fitting generalized Maxwell model for rubber to experimental data at
 $T = 20\text{ }^{\circ}\text{C}$

Viscoelastic sliding: bulk friction



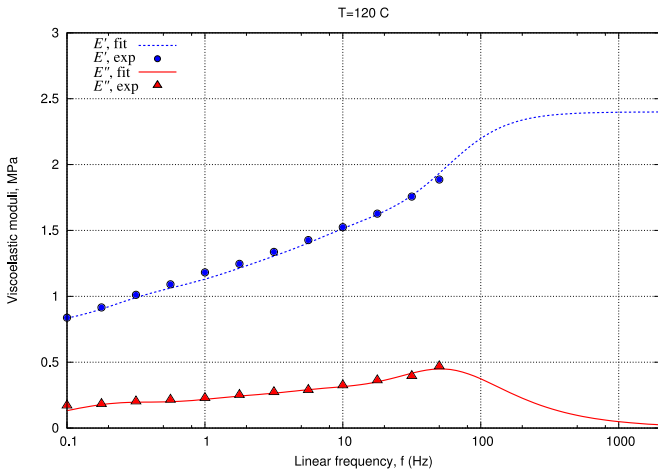
Fitting generalized Maxwell model for rubber to experimental data at
 $T = 80 \text{ } ^\circ\text{C}$

Viscoelastic sliding: bulk friction



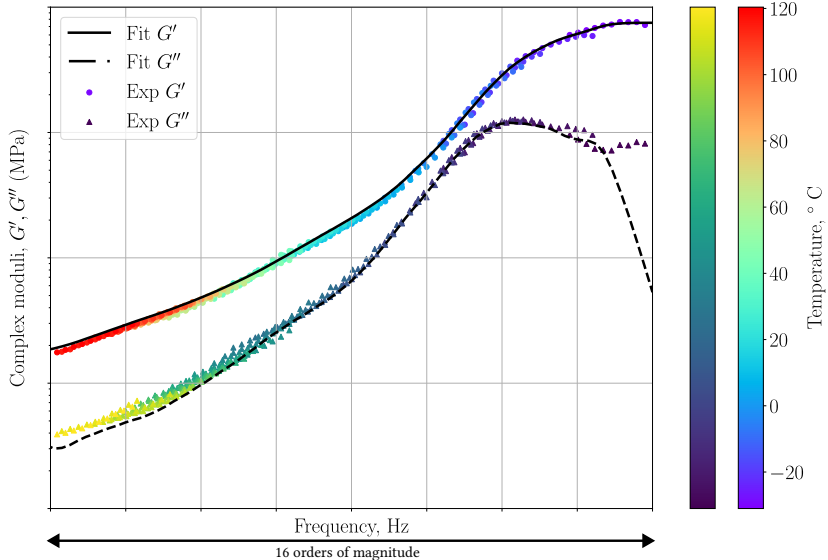
Fitting generalized Maxwell model for rubber to experimental data at
 $T = 100\text{ }^{\circ}\text{C}$

Viscoelastic sliding: bulk friction



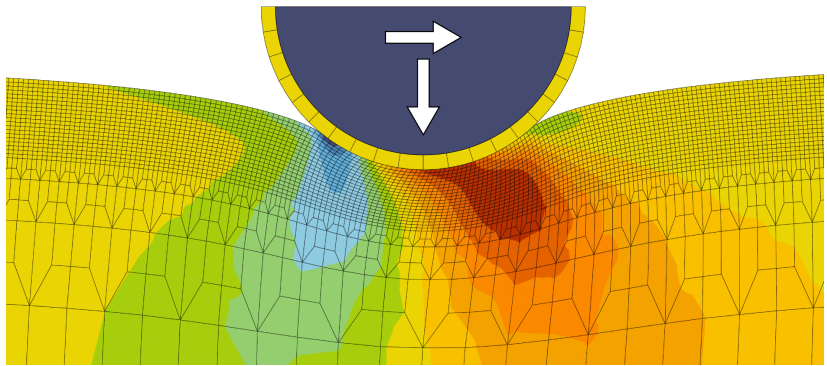
Fitting generalized Maxwell model for rubber to experimental data at
 $T = 120\text{ }^{\circ}\text{C}$

Viscoelastic sliding: bulk friction



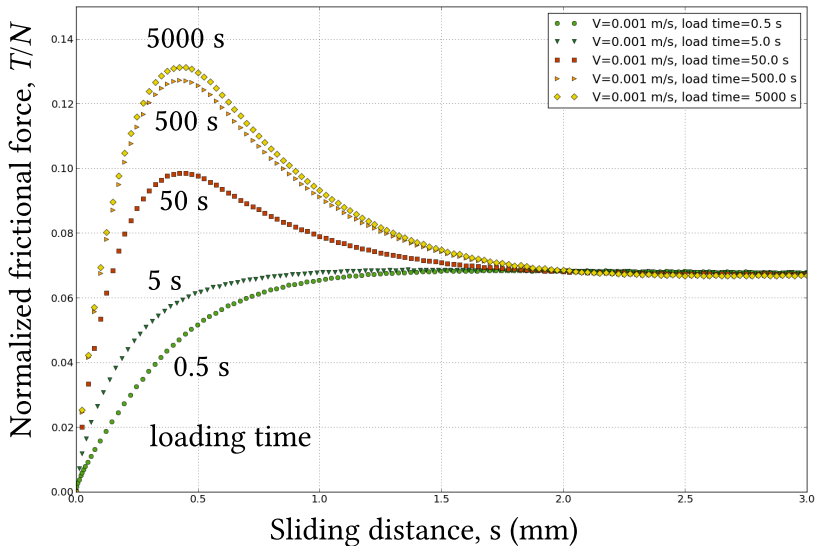
Full data on complex moduli of a sample charged rubber

Viscoelastic sliding: bulk friction



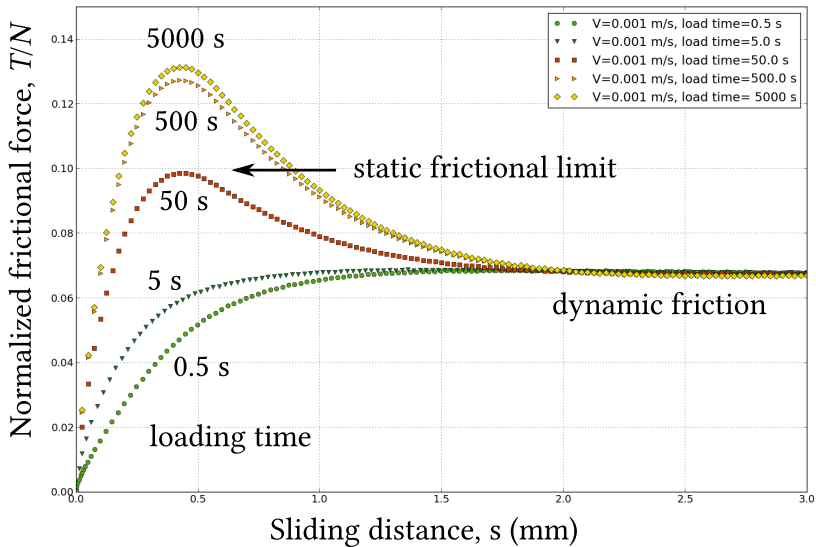
Simulation sketch

Viscoelastic sliding: bulk friction



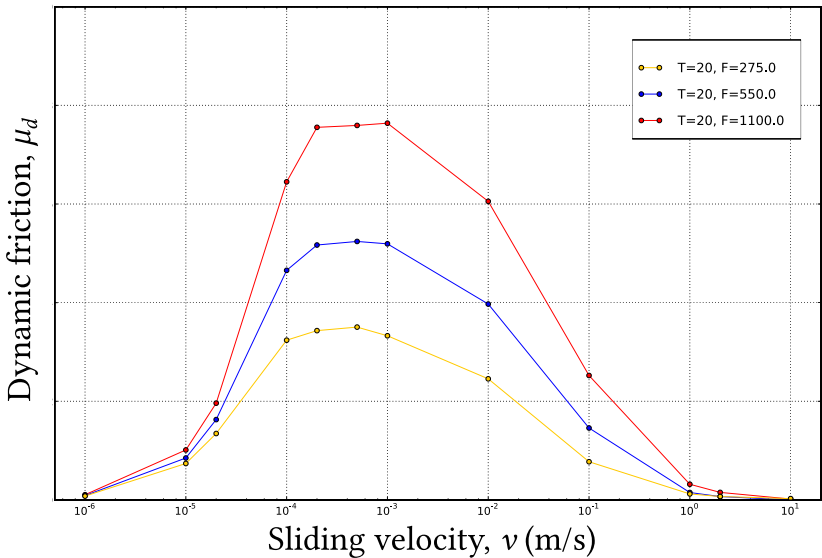
Effect of normal-loading rate on the frictional force evolution

Viscoelastic sliding: bulk friction



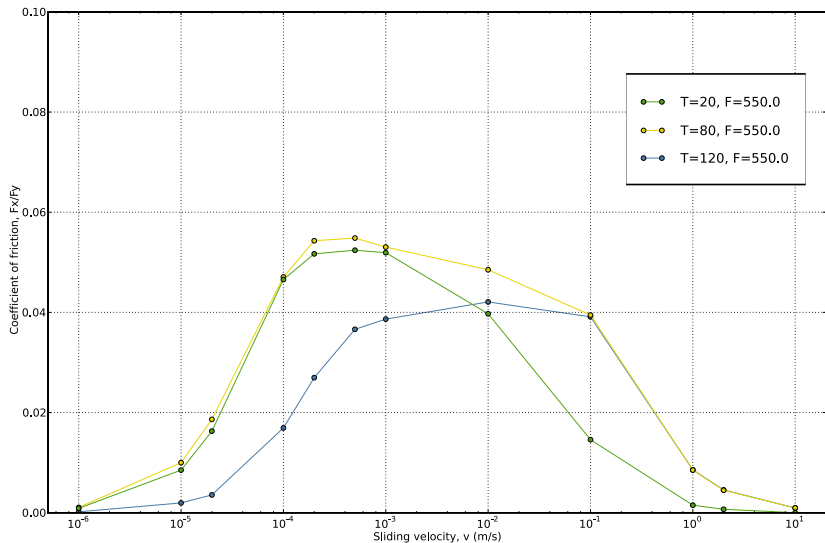
Effect of normal-loading rate on the frictional force evolution

Viscoelastic sliding: bulk friction



Frictional force at different slip velocity (effect of force)

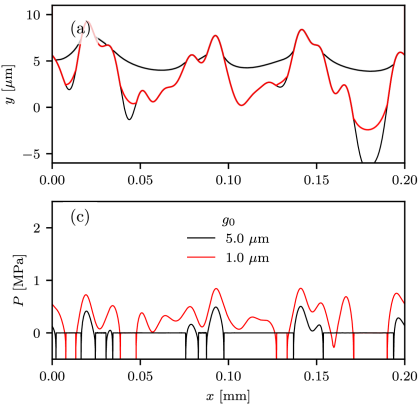
Viscoelastic sliding: bulk friction



Frictional force at different slip velocity (effect of temperature)

Viscoelastic friction: recent progress

- Account for multiscales^[1,2]
- Account for adhesion^[1,2]
- Account for large deformations^[3]

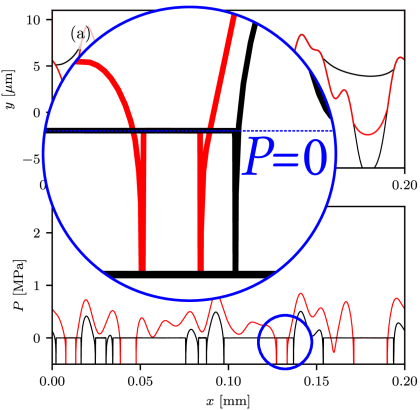


Simulation results^[1]

- [1] Plagge, J. and Hentschke, R., (2022) Numerical solution of the adhesive rubber-solid contact problem and friction coefficients using a scale-splitting approach. *Tribology International*, 173:107622.
- [2] Carbone, G., Mandriota, C. and Menga, N., (2022) Theory of viscoelastic adhesion and friction. *Extreme Mechanics Letters*, 56:101877.
- [3] Lengiewicz, J., de Souza, M., Lahmar, M.A., Courbon, C., Dalmas, D., Stupkiewicz, S. and Scheibert, J., (2020) Finite deformations govern the anisotropic shear-induced area reduction of soft elastic contacts. *Journal of the Mechanics and Physics of Solids*, 143:104056

Viscoelastic friction: recent progress

- Account for multiscales^[1,2]
- Account for adhesion^[1,2]
- Account for large deformations^[3]

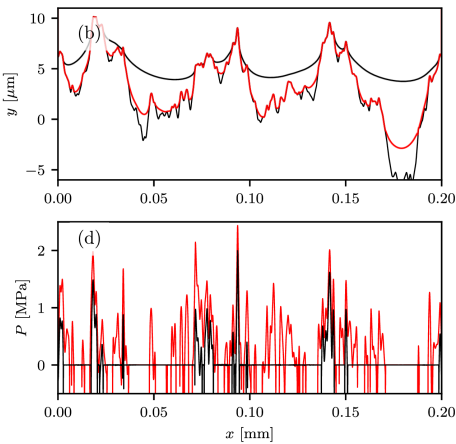


Simulation results^[1]

- [1] Plagge, J. and Hentschke, R., (2022) Numerical solution of the adhesive rubber-solid contact problem and friction coefficients using a scale-splitting approach. *Tribology International*, 173:107622.
- [2] Carbone, G., Mandriota, C. and Menga, N., (2022) Theory of viscoelastic adhesion and friction. *Extreme Mechanics Letters*, 56:101877.
- [3] Lengiewicz, J., de Souza, M., Lahmar, M.A., Courbon, C., Dalmas, D., Stupkiewicz, S. and Scheibert, J., (2020) Finite deformations govern the anisotropic shear-induced area reduction of soft elastic contacts. *Journal of the Mechanics and Physics of Solids*, 143:104056

Viscoelastic friction: recent progress

- Account for multiscales^[1,2]
- Account for adhesion^[1,2]
- Account for large deformations^[3]



Simulation results^[1]

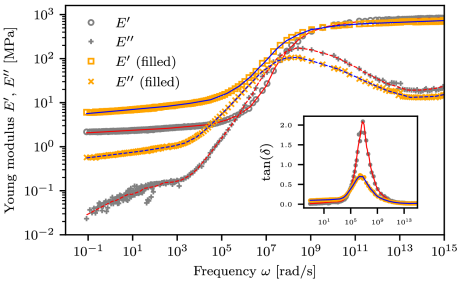
[1] Plagge, J. and Hentschke, R., (2022) Numerical solution of the adhesive rubber-solid contact problem and friction coefficients using a scale-splitting approach. *Tribology International*, 173:107622.

[2] Carbone, G., Mandriota, C. and Menga, N., (2022) Theory of viscoelastic adhesion and friction. *Extreme Mechanics Letters*, 56:101877.

[3] Lengiewicz, J., de Souza, M., Lahmar, M.A., Courbon, C., Dalmas, D., Stupkiewicz, S. and Scheibert, J., (2020) Finite deformations govern the anisotropic shear-induced area reduction of soft elastic contacts. *Journal of the*

Viscoelastic friction: recent progress

- Account for multiscales^[1,2]
- Account for adhesion^[1,2]
- Account for large deformations^[3]



Simulation results^[1]

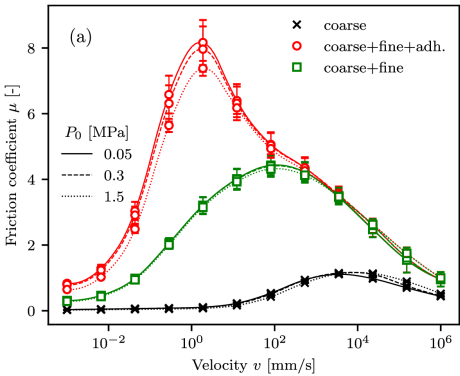
[1] Plagge, J. and Hentschke, R., (2022) Numerical solution of the adhesive rubber-solid contact problem and friction coefficients using a scale-splitting approach. *Tribology International*, 173:107622.

[2] Carbone, G., Mandriota, C. and Menga, N., (2022) Theory of viscoelastic adhesion and friction. *Extreme Mechanics Letters*, 56:101877.

[3] Lengiewicz, J., de Souza, M., Lahmar, M.A., Courbon, C., Dalmas, D., Stupkiewicz, S. and Scheibert, J., (2020) Finite deformations govern the anisotropic shear-induced area reduction of soft elastic contacts. *Journal of the Mechanics and Physics of Solids*, 143:104056

Viscoelastic friction: recent progress

- Account for multiscales^[1,2]
- Account for adhesion^[1,2]
- Account for large deformations^[3]



Simulation results^[1]

[1] Plagge, J. and Hentschke, R., (2022) Numerical solution of the adhesive rubber-solid contact problem and friction coefficients using a scale-splitting approach. *Tribology International*, 173:107622.

[2] Carbone, G., Mandriota, C. and Menga, N., (2022) Theory of viscoelastic adhesion and friction. *Extreme Mechanics Letters*, 56:101877.

[3] Lengiewicz, J., de Souza, M., Lahmar, M.A., Courbon, C., Dalmas, D., Stupkiewicz, S. and Scheibert, J., (2020) Finite deformations govern the anisotropic shear-induced area reduction of soft elastic contacts. *Journal of the Mechanics and Physics of Solids*, 143:104056

Time-Dependent Friction

Check a separate presentation



Thank you for your attention!